


Article

# Stable Isotope Hydrology of Cave Groundwater and Its Relevance for Speleothem-Based Paleoenvironmental Reconstruction in Croatia

Maša Surić <sup>1,\*</sup> , György Czuppon <sup>2,3</sup>, Robert Lončarić <sup>1</sup> , Neven Bočić <sup>4</sup> , Nina Lončar <sup>1</sup> , Petra Bajo <sup>5</sup> and Russell N. Drysdale <sup>6,7</sup>

<sup>1</sup> Department of Geography, Center for Karst and Coastal Research, University of Zadar, 23000 Zadar, Croatia; rloncar@unizd.hr (R.L.); nloncar@unizd.hr (N.L.)

<sup>2</sup> Institute for Geological and Geochemical Research, RCAES, H-1112 Budapest, Hungary; czuppon@geochem.hu

<sup>3</sup> Department of Hydrogeology and Engineering Geology, Institute of Environmental Management, University of Miskolc, H-3515 Miskolc, Hungary

<sup>4</sup> Department of Geography, Faculty of Science, University of Zagreb, 10000 Zagreb, Croatia; nbocic@geog.pmf.hr

<sup>5</sup> Croatian Geological Survey, 10000 Zagreb, Croatia; pbajo@hgi-cgs.hr

<sup>6</sup> School of Geography, Faculty of Science, The University of Melbourne, 3010 Melbourne, Australia; rnd@unimelb.edu.au

<sup>7</sup> Laboratoire EDYTEM (UMR CNRS 5204), Université de Savoie-Mont Blanc, 73000 Chambéry, France

\* Correspondence: msuric@unizd.hr

Received: 24 July 2020; Accepted: 23 August 2020; Published: 25 August 2020



**Abstract:** Speleothems deposited from cave drip waters retain, in their calcite lattice, isotopic records of past environmental changes. Among other proxies,  $\delta^{18}\text{O}$  is recognized as very useful for this purpose, but its accurate interpretation depends on understanding the relationship between precipitation and drip water  $\delta^{18}\text{O}$ , a relationship controlled by climatic settings. We analyzed water isotope data of 17 caves from different latitudes and altitudes in relatively small but diverse Croatian karst regions in order to distinguish the dominant influences. Drip water  $\delta^{18}\text{O}$  in colder caves generally shows a greater resemblance to the amount-weighted mean of precipitation  $\delta^{18}\text{O}$  compared to warmer sites, where evaporation plays an important role. However, during glacial periods, today's 'warm' sites were cold, changing the cave characteristics and precipitation  $\delta^{18}\text{O}$  transmission patterns. Superimposed on these settings, each cave has site-specific features, such as morphology (descending or ascending passages), altitude and infiltration elevation, (micro) location (rain shadow or seaward orientation), aquifer architecture (responsible for the drip water homogenization) and cave atmosphere (governing equilibrium or kinetic fractionation). This necessitates an individual approach and thorough monitoring for best comprehension.

**Keywords:** stable isotopes; drip water; speleothem; cave; Croatia

## 1. Introduction

Understanding the mechanisms and extent of past environmental changes is a key consideration for predicting global climate changes. Most impacted and potentially endangered is Earth's Critical Zone (ECZ), the thin surface zone that extends from the upper limit of vegetation to the lower limit of groundwater bodies in which coupled chemical, biological, physical, and geological processes operate together to sustain life [1]. This is an extremely heterogeneous zone whose natural functioning is strongly regulated by climate, i.e., changes in temperature and hydrology and their influence on vegetation

and soil evolution [2]. One of the natural archives which confidentially record hydroclimate changes in ECZ are speleothems—secondary carbonate deposits that precipitate in a cave environment from groundwaters (cave drip water) supersaturated with respect to calcite following CO<sub>2</sub>-driven dissolution of carbonate bedrock [3]. The importance of speleothems for paleoenvironmental reconstructions through the use of stable isotopes was recognized in the 1960's [4], especially the ability of δ<sup>18</sup>O to record cave temperature variations [5]. In the following decades, various other proxies have emerged, such as trace elements (Mg, Sr, Y, Pb, Zn, P, U), organic acids, lipid biomarkers, magnetic susceptibility, laminae thickness and growth rate variations, along with development of very precise and accurate dating techniques (U-Th, U-Pb), which have given great momentum to speleothem science. It has been suggested that, after the dominance of ice and deep-sea cores, the future in Quaternary paleoclimate studies might belong to speleothem science [6].

Where equilibrium deposition can be demonstrated, speleothem δ<sup>18</sup>O depends solely on cave air temperature and drip water δ<sup>18</sup>O [5,7]. Establishing cave hydroclimate monitoring is critical to assess variability in these two parameters. Although it is not always the case [8], caves are usually considered environments with stable microclimate parameters, with relative humidity (RH) close to 100%, and air temperature equal to the surface mean annual air temperature (MAAT), without seasonal variations. When such conditions are met in particular parts of the cave, underground environmental changes respond to long-term climate changes and are recorded in the isotopic composition of slow-growing speleothems. However, successful interpretation of speleothem records depends on comprehension of the spatial and temporal variability of drip water hydrology and composition [9,10] as the water undergoes complex processes on its way from the atmosphere, through the soil and epikarst and to the cave, with final temperature-dependent fractionation and incorporation into the speleothem calcite lattice [11,12].

Croatia's central position between the western and eastern Mediterranean, at the interface of continental European and maritime Mediterranean influences, together with its variety of landscapes, makes this region interesting in terms of paleoclimate and paleoenvironmental studies based on different approaches and archives, such as: loess sequences, [13–16] lake sediments, [17–20], marine and transitional deposits, [21–23], algal rims [24] and speleothems (see an overview in [25] and references therein). Speleothem-based studies require insight into atmospheric isotope patterns from global to local scale, and variations in precipitation isotope composition in Croatia on a local and regional scale have been discussed in Krajcar Bronić et al., [26–28], Horvatinčić et al., [29,30], Barešić et al., [31] and Vreča et al., [32]. Regional isotopic signatures of groundwater from ca. 100 sites in Croatia and their relationship to precipitation are discussed in Brkić et al., [33].

Here we discuss the outcomes of several cave drip water research campaigns. We examine the response of each cave system to surface precipitation and the transmission of the isotopic signals that are ultimately captured in the speleothems as environmental records. The study encompasses 17 sites with elevations from 32 m to 1550 m above sea level (a.s.l.) and four different climate types (Cfa—temperate with hot summer; Cfb—temperate with warm summer; Csa—temperate dry with hot summers; Df—cold and wet continental, according to Köppen-Geiger climate classification [34]), covering most of the Croatian karst regions. The studies can be divided into three groups according to their duration:

- Systematic sampling with at least one-year of continuous monitoring and monthly sampling of rain and drip water was applied within three research projects that included Manita peć (MP), Strašna peć (SP) and Špilja u Zubu Buljme (ZB) caves [35]; Upper Barač (GB), Lower Barač (DB) and Lower Cerovačka (DC) caves [36]; and Nova Grgosova (NG), Lokvarka (LOK) and Modrič (MOD) caves [37,38].
- Semi-continuous sampling was performed in a study of the Velebita Cave System (VEL), and the Sirena (SIR) and Lukina jama (LUK) pits [39].
- Sporadic and one-off sampling occurred in Medvjeđa špilja (MED), Špilja u Vrdolju (VRD), Kraljičina Špilja (KRA), Strašna peć, Mala špilja (MML) and Velika špilja (VML) caves [40–42], and Modrič Cave [43].

We investigated the dominant factors controlling the transmission of the isotopic signal from precipitation to cave drip water in different climate settings, and how this information can be interpreted in speleothem-based climate reconstructions.

## 2. Study Area

A total of 43.7% of the Croatian territory is covered by karst [44]. The northern and eastern parts of the country are characterized by several isolated karst patches, while practically the whole western and southern parts belong to the Dinaric classical karst, extending parallel to the eastern Adriatic coast (Figure 1). Due to the temperate location (between 42.2 and 46.2° N) with sufficient precipitation year round (700–3000 mm), tectonically fractured carbonate bedrock has undergone extensive karstification, resulting in the development of a large range of surface and underground karst features, including karst hydrogeology. According to a karst landscape definition based on altitude range and climate (aridity index and mean annual days with snow cover), three (out of four) karst landscapes intertwine in this small region of Croatia: humid hills and plains, Mediterranean medium range mountains and high range mountains (see Figure 4 in [45]).

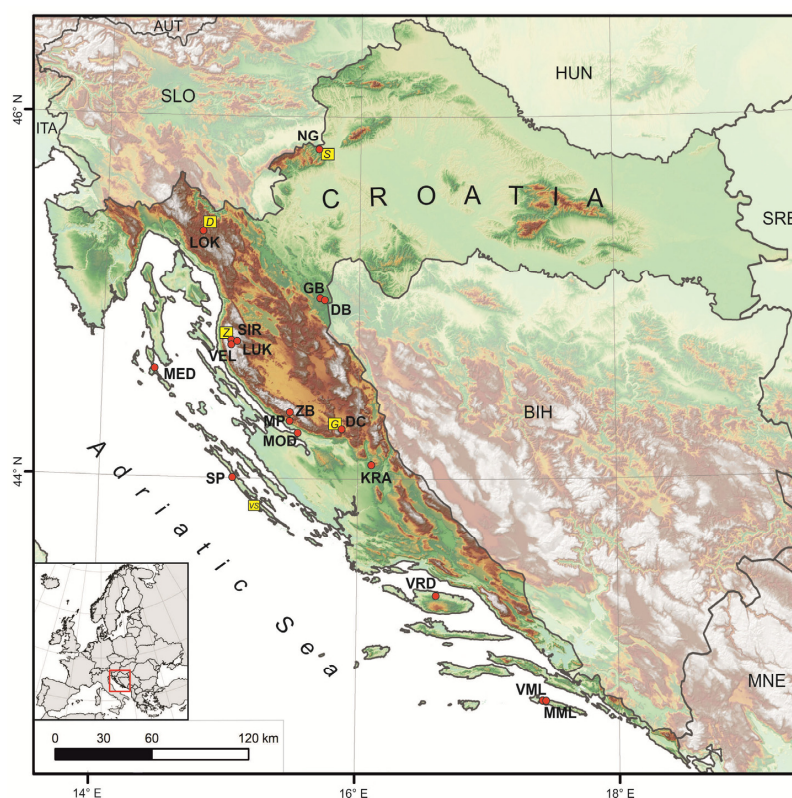


**Figure 1.** Study area with cave locations: NG—Nova Grgosova, LOK—Lokvarka, GB—Upper Barač, DB—Lower Barač, SIR—Sirena, LUK—Lukina jama, VEL—Velebita, MED—Medvjeđa špilja, ZB—Špilja u Zubu Buljme, MP—Manita peč, DC—Lower Cerovačka, MOD—Modrič, KRA—Kraljičina špilja, SP—Strašna peč, VRD—Špilja u Vrdoļu, VML—Velika špilja, MML—Mala špilja. Yellow squares denote meteorological station: S—Samobor 141 m a.s.l., D—Delnice (681 m a.s.l.), Z—Zavižan (1594 m a.s.l.), G—Gračac (567 m a.s.l.), VS—Vela Sestrica (35 m a.s.l.).

Unofficially, over 10,000 caves are already known in Croatia [46], but this figure is in reality much higher as caves have been discovered in all carbonate geological units, from Upper Palaeozoic to the Neogene. The studied caves (Table 1) can be divided into several groups according to their geographical position and associated climate conditions (Figure 2), which do not necessarily imply similar environmental settings of relatively adjacent caves. Most similar are the shallow and low-altitude caves located on the

islands and along the coast (MOD, SP, MED, VRD, KRA, MML, VML), then high-mountain caves (ZB, VEL, SIR, LUK) and mid-altitude continental caves which have site-specific climatic settings, regardless of their relative vicinity (NG, LOK, DB, GB, DC). MP cave is, according to its latitude and altitude (570 m a.s.l.), expected to be the most similar to DC cave, but its location on the south-western slopes of the Velebit Mt. makes it more similar to the coastal sites.

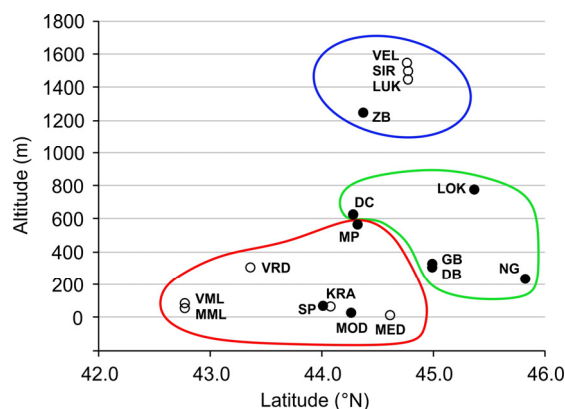


**Figure 2.** Altitudinal and latitudinal distribution of studied caves clustered according to general climate similarity—coastal and island caves (red), continental mid-altitude caves (green) and high-mountain caves (blue). Closed circles denote caves with systematic monitoring/sampling, while open circles represent caves with sporadic sampling.

Climate and weather patterns over the study area are governed by the seasonal presence of the various pressure systems and air masses. During the summer, the influence of the Azores High prevails in the coastal region and causes dry weather along most of the Croatian coast, while continental Croatia is more susceptible to intrusions of cooler and moist air masses from the Atlantic. During winter, the continental part is often under the influence of Siberian High, which produces cold and dry weather; the coast is under the influence of low pressure systems originating either from the Atlantic Ocean, the Mediterranean or the Adriatic Sea.

Although the study sites are located relatively close to each other, they exhibit quite different climate properties, particularly seasonal precipitation distribution. Most of the locations have precipitation maxima in autumn (October and November) due to the frequent passage of frontal systems within atmospheric lows, with the exception of low-altitude sites in continental Croatia, i.e., NG cave (represented by data from the Samobor meteorological station, Figure 3), which has maximum precipitation in the late summer caused by the combined effect of convective and frontal rain. Sites located in the continental regions, but at higher altitudes (LOK cave represented by the Delnice station), exhibit orographic effects, which cause a surge in the precipitation amount (annual precipitation in Delnice is 2218 mm compared to 1073 mm in Samobor). A similar effect is present in the high-altitude sites (ZB, VEL, SIR, LUK caves, represented by the data from Zavižan station), but with slightly lower precipitation due to the lower air temperatures (MAAT of 5.0 °C Zavižan, and 8.4 °C in Delnice). On the other hand, sites on the leeward side of the mountains (DB, GB, DC caves) tend to have somewhat decreased precipitation probably due to their locations in the rain shadow. Coastal and island sites SP, KRA, VRD, VML and MML (represented by Vela Sestrica station) have a typical Mediterranean precipitation distribution with pronounced summer droughts (Csa) and low overall precipitation amounts (666 mm), while MOD, MED and MP caves receive more precipitation than other coastal sites and summer droughts are less pronounced (Cfa). MP cave is also unusual on account of the relatively large difference between its surface MAAT (13.7 °C in 2014–2015 and 14.8 °C in 2018–2020) and a cave MAAT of 9.0 °C ( $1\sigma = 0.4$ ) in 2012–2014. This is a consequence of cave morphology, i.e., descending chambers acting as a ‘cold trap’ [35]. Thus, it can be regarded as a transitional cave with climatic properties of both coastal and continental sites, as it has average summer temperatures higher than the continental sites, but also more precipitation than other coastal sites.

**Table 1.** Geographical positions of the caves, average cave air temperature, climate type of the cave region, monitoring and sampling periods and number of drip water samples. Colours of climate types correspond with the colours of the cave clusters in Figure 2. Monthly integrated drip water samples are given in bold and same locations have undergone systematic monitoring with monthly integrated rainwater sampling. Temperatures marked with (\*) are averaged from [36] and [47] and with (\*\*) are marked temperature ranges of deep vertical caves (see [48–51] for details).

Cave	Location	Acronym	Entrance			Clim. Type	Aver. Temp. (°C)	Monitoring/Sampling Period	Number of Drip Water Samples	Ref.
			Lat. (N)	Long. (E)	Alt. (m)					
Nova Grgosova	Samobor Hills	NG	45°49′	15°41′	239	Cfb	11.2	November 2014–November 2015	<b>36</b>	[25]
Lokvarka	Gorski Kotar	LOK	45°22′	14°46′	780	Cfb	7.5	November 2014–November 2015	<b>24</b>	[25]
Gornja Baračeva	Kordun	GB	44°59′	15°43′	331.5	Cfb	10.2*	April 2013–July 2014	<b>24</b>	[36]
Donja Baračeva	Kordun	DB	44°59′	15°43′	309.5	Cfb	10.1 *	April 2013–July 2014	<b>28</b>	[36]
Sirena	N Mt Velebit	SIR	44°46′	14°59′	1500	Df	1.7–3.6 **	2 August 2013	1	[39]
Lukina jama	N Mt Velebit	LUK	44°46′	15°02′	1450	Df	0–5 **	5 August 2013	1	[39]
Velebita Cave System	N Mt Velebit	VEL	44°45′	14°59′	1550	Df	3.5–5.5 **	31 July 2012–4 August 2013 1 August 2013	18	[39]
Medvjeda špilja	Lošinj Island	MED	44°36′	14°24′	17.5	Cfa	15	13 December 2009–10 January 2010	1	[41]
Špilja u Zubu Buljme	S Mt Velebit	ZB	44°22′	15°28′	1250	Df	4.0	July 2012–July 2013	<b>11</b>	[35]
Manita peć	S Mt Velebit	MP	44°19′	15°29′	570	Cfa	9.0	July 2012–July 2013	<b>32</b>	[35]

Table 1. Cont.

Cave	Location	Acronym	Entrance			Clim. Type	Aver. Temp. (°C)	Monitoring/Sampling Period	Number of Drip Water Samples	Ref.
			Lat. (N)	Long. (E)	Alt. (m)					
Donja Cerovačka	Lika	DC	44°16′	15°53′	630	Cfb	6.8	April 2013–January 2015	21	[36]
Modrič	Mt Velebit foothill	MOD	44°15′	15°32′	32	Cfa	16.6	June 2007–September 2007	3	[43]
								July 2007–May 2008	1	
								November 2007–May 2008	1	
								June 2008–September 2010	54	
November 2014–November 2018	93	[25]								
Kraljičina špilja	Vis Island	KRA	44°04′	16°06′	70	Csa	14.1	19–20 May 2010	1	[41]
Strašna peć	Dugi otok Island	SP	44°00′	15°02′	74	Csa	11.1	20 June–29 September 2010	2	[41]
								July 2012–January 2014	36	[35]
Špilja u Vrdolju	Brač Island	VRD	43°21′	16°36′	310	Csa	13.5	18–19 May 2010	1	[41]
Velika špilja	Mljet Island	VML	42°46′	17°28′	90	Csa	14	20–22 February 2010	2	[41]
Mala špilja	Mljet Island	MML	42°46′	17°29′	60	Csa	13	20–22 February 2010	1	[41]

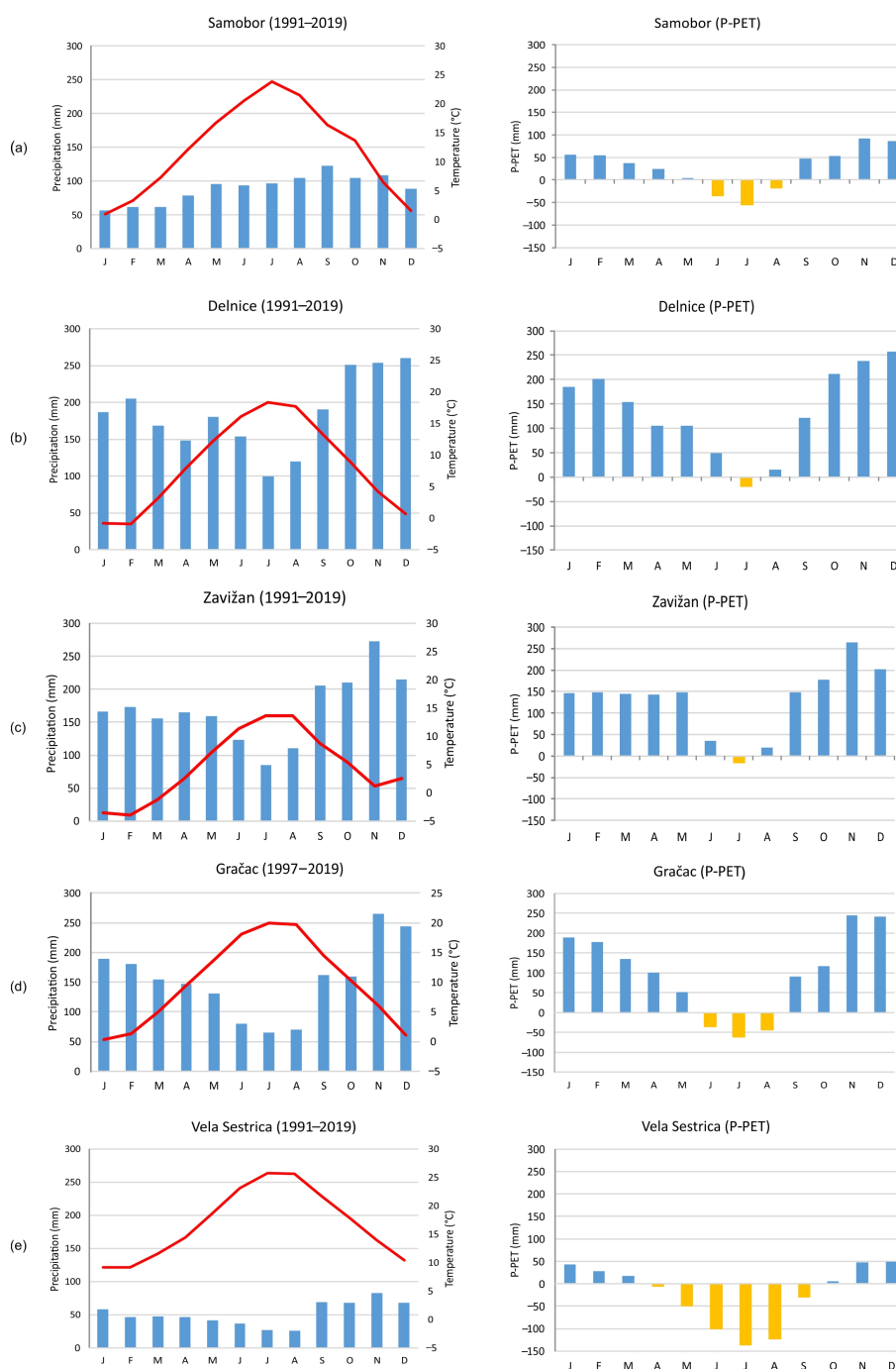


**Figure 3.** Climate data (left: air temperature and precipitation; right: difference between precipitation and potential evapotranspiration) for five characteristic regions: (a) Samobor station representing continental NG cave; (b) Delnice station representing continental settings with orographic effect on LOK cave; (c) Zavižan station for high-altitude conditions with a strong orographic effect (ZB, VEL, SIR, LUK); (d) Gračac station as representative for continental sites with a rain-shadow effect (DB, GB, DC caves); and (e) Vela Sestrica station representing conditions of low-altitude caves located on the islands and along the coast (MOD, SP, MED, VRD, KRA, MML, VML). Data obtained from the Croatian Meteorological and Hydrological Service [52]. Locations of the meteorological stations are given in Figure 1. Water balance (potential evapotranspiration) is calculated using the Thornthwaite evapotranspiration model [53,54].

### 3. Monitoring and Sampling Methodology

An overview of monitoring duration and number of samples is given in Table 1. Monitoring and sampling practice for the systematic long-term studies (NG, LOK, MOD, ZB, MP, SP, DB, GB, DC caves) was the same at all sites, and included recording meteorological parameters (air temperature and relative humidity) outside and inside the caves and measuring the isotopic composition ( $\delta^2\text{H}$  and  $\delta^{18}\text{O}$ ) of rain and cave drip water [25,35,36]. Additionally, analyses of drip water elemental composition were performed at DB and GB sites [36] and in MOD cave (2012–2013, unpublished), while in NG, LOK, MOD, ZB, MP and SP caves drip intensity was recorded [25,35].

Microclimate data were measured at one-hour resolution by HOBO U23 Pro v2 Temperature/Relative Humidity Data Loggers. Loggers were mounted at 1.5–2.0 m above the cave floor and 2–3 cm off the wall to avoid recording the thermal signal of the bedrock, which is delayed, usually dampened [55] and could be misleading.

Monthly-integrated rainwater samples have been collected above ZB, MP, SP [35] NG, LOK and MOD caves [25] in plastic containers with funnel protected by PVC net to prevent clogging and a layer of paraffin oil to hamper the evaporation of collected rainwater, as this significantly effects water isotopic composition. During the study of MOD cave by Rudzka et al., [37], a Pluvimate<sup>®</sup> rain-gauge was used in order to collect rainwater and record its intensity. At the GB/DB and DC sites composite monthly samples of precipitation were collected by simple anti-evaporation system without an oil film, while at VEL, SIR and LUK sites the system of Gröning et al. [56] was employed [39]. Daily precipitation amount data were obtained from adjacent meteorological stations operated by the Croatian Meteorological and Hydrological Service (CMHS).

Monthly-integrated drip water samples were collected under the drip sites that had been feeding stalagmites predetermined for paleoclimate studies in NG, LOK, MOD, ZB, MP, SP, DB, GB, DC, as well as from several other drip points. In-cave water containers did not include protective paraffin oil since the cave air RH was 100%, as anticipated, so no evaporation was expected. It has also been empirically proven that equilibration of the collected water with the moisture of the cave atmosphere takes approximately three months [57], i.e., collected drip water samples would not have been compromised within one month. Regardless of the negative water balance during the summer season (especially pronounced in coastal region, e.g., Vela Sestrica station in Figure 3), it must be emphasized that practically all our drip sites had continuous discharge all year round. Research in the high-mountain Velebita Cave System (VEL), which is a 1026 m deep vertical cave, focused on the isotopic composition variability along a vertical profile and its comparison with two other pits (LUK and SIR), with local precipitation and with some remote spring waters. Thus, along the VEL profile, 1 to 6 samples were collected daily during five days of caving, while in LUK and SIR only one sample of water in each cave was collected [39]. In island caves (SP, MED, VRD, KRA, MML, VML) the single samples were also collected per drip site, with drip water accumulating from 2 to 102 days [40,41]. All drip water samples were taken from the exact sites from where speleothems have been collected for paleoenvironmental reconstruction.

Modern calcite was collected on pre-cleaned glass plates (10 × 10 cm) in MP caves, on plastic funnels and glass plates in SP cave [35] and on a nylon sheet in MOD cave [43]. Farming of modern calcite in DB and GB caves was performed by placing light bulbs under active drip sites, imitating the rounded stalagmite surface [36]. We avoided sampling of the youngest parts of the active stalagmites since with the artificial material we were sure about the period of deposition. Analytical methods related to stable isotope measurements used in Rudzka et al., [37], Lončar [40], Surić et al., [25,35], Czuppon et al., [36] and Paar et al. [39] are given in detail in Appendix A.

Valuable information on aquifer architecture can be obtained from the relationship between precipitation and cave discharge [58], so NG, LOK, MOD, ZB, MP and SP caves were also equipped with automated acoustic Stalagmate<sup>®</sup> drip counters [59] to record discharge dynamics.



#### 4. Results and Discussion

A statistical summary of the  $\delta^{18}\text{O}$  and  $\delta^2\text{H}$  data from the majority of analyzed water samples is given in Tables 2 and 3. Systematic monitoring and sampling of precipitation revealed nine local meteoric water lines (LMWL) (linear regression between precipitation  $\delta^{18}\text{O}$ - $\delta^2\text{H}$  monthly values) (Figure 4) along which corresponding cave drip water  $\delta^{18}\text{O}$ - $\delta^2\text{H}$  values are distributed according to different site-specific environmentally dependent patterns. The relationship between the isotopic composition of precipitation and cave drip water is presented in Figures 5–7, and spatiotemporal patterns of precipitation isotopic signal transmitted to the cave drip water are discussed in the following sections.

**Table 2.** Minimum, maximum and amplitude of precipitation and drip water  $\delta^{18}\text{O}$  and  $\delta^2\text{H}$  from NG, LOK, MP, GB, DB, ZB, MP, DC, MOD and SP caves for the periods given in Table 1. Sites are arranged by latitude. All the values are given in ‰ with respect to Vienna Standard Mean Ocean Water VSMOW.

Cave	Precipitation						Drip Site	Drip Water					
	Maximum		Minimum		Amplitude			Maximum		Minimum		Amplitude	
	$\delta^{18}\text{O}$	$\delta^2\text{H}$	$\delta^{18}\text{O}$	$\delta^2\text{H}$	$\delta^{18}\text{O}$	$\delta^2\text{H}$		$\delta^{18}\text{O}$	$\delta^2\text{H}$	$\delta^{18}\text{O}$	$\delta^2\text{H}$	$\delta^{18}\text{O}$	$\delta^2\text{H}$
NG	−4.6	−24.6	−13.5	−93.5	8.9	68.9	NG-1W	−9.5	−63.1	−10.1	−65.8	0.6	2.7
							NG-2W	−9.6	−63.3	−10.0	−65.6	0.4	2.3
							NG-3W	−9.6	−63.1	−9.9	−64.1	0.3	1.0
LOK	−5.3	−29.0	−13.9	−96.8	8.6	67.8	LOK-1W	−7.9	−45.9	−9.7	−58.5	1.3	12.6
							LOK-2W	−8.5	−50.2	−8.8	−52.1	0.3	1.9
GB/DB	−5.4	−34.6	−12.9	−86.8	7.5	52.2	GB-1	−9.5	−64.0	−11.0	−74.2	1.5	10.2
							GB-2	−10.2	−70.7	−11.8	−82.0	1.6	11.3
							DB-1	−10.0	−70.7	−11.1	−77.1	1.1	6.4
							DB-2	−10.0	−71.5	−10.8	−74.2	0.8	2.7
ZB	−5.9	−30.9	−13.4	−93.2	7.5	62.3	ZBW	−7.4	−41.2	−8.2	−48.4	0.8	7.2
MP	−3.4	−16.3	−9.4	−58.9	6.0	42.6	MP-1W	−6.3	−36.1	−7.9	−48.4	1.6	12.3
							MP-2W	−6.6	−36.3	−7.5	−43.1	0.9	6.8
							MP-3W	−6.4	−33.3	−7.7	−47.9	1.3	14.6
DC	−5.3	−32.3	−10.7	−73.9	5.4	41.6	DC-2	−7.5	−46.0	−8.4	−51.8	0.9	5.8
MOD	−3.2	−17.0	−8.6	−57.1	5.4	40.1	MOD-21W	−5.7	−33.6	−6.8	−41.7	1.1	8.1
							MOD-22W	−3.9	−17.0	−6.0	−35.3	2.1	18.3
							MOD-31W	−5.6	−34.1	−6.3	−38.6	0.7	4.5
							MOD-32W	−5.9	−35.7	−6.4	−38.8	0.5	3.1
SP	−3.8	−23.2	−8.3	−50.6	4.5	27.4	SP1W	−6.0	−32.3	−6.8	−35.8	0.8	3.5
							SPNW	−6.2	−33.2	−6.7	−38.8	0.5	5.6

##### 4.1. Moisture Sources Affecting Isotopic Composition

The aim of many speleothem-based studies is to assess past dynamics of atmospheric water vapor masses e.g., [60–63], as their shifts have governed associated precipitation, temperature and vegetation distribution. Of special interest are bordering regions such as the one between continental European and Mediterranean influences, and in that sense the Croatian region could play an important role, since this spatially small area rich in geographical and climatic variety is presently characterized by complex patterns of precipitation isotopes [26,27,32,35]. Figure 4 shows regression lines of nine sets of precipitation data. Since some of the lines are based on one year of data, the  $R^2$  is given to depict statistically significant correlations. The most obvious characteristic of this set of LMWLs is their departure from the Eastern Mediterranean meteoric water line (EMMWL:  $\delta^2\text{H} = 8 \times \delta^{18}\text{O} + 22$  [64]) which represents environments characterized by substantial evaporation under conditions of a large humidity deficit [65]. This is apparently not the case in our studied region. The LMWLs are generally clustered along the Global meteoric water line (GMWL:  $\delta^2\text{H} = 8 \times \delta^{18}\text{O} + 10$  [66]) and the western Mediterranean meteoric water line (WMMWL:  $\delta^2\text{H} = 8 \times \delta^{18}\text{O} + 13.7$  [67]), which marks the transitional

zone with mixing influences of warm eastern Mediterranean and cool North Atlantic air masses [67]. Another characteristic of these water lines are the slopes, which are systematically lower (from 6.6 to 7.8) than that of the GMWL, with a distinct difference between northern continental stations (closer to the GMWL slope), and maritime sites with lower values. The reason for this is secondary evaporation which occurs as rain falls through a dry air column above the ground and leads to kinetic fractionation [68]. This is a typical situation during the coastal dry and hot summers (Figure 3e), while the uniform annual distribution of the precipitation partially suppresses that effect in continental sites (Figure 3a,b). However, it is obvious that all caves receive mixed precipitation from the Atlantic and Mediterranean regions, but with different seasonal patterns.

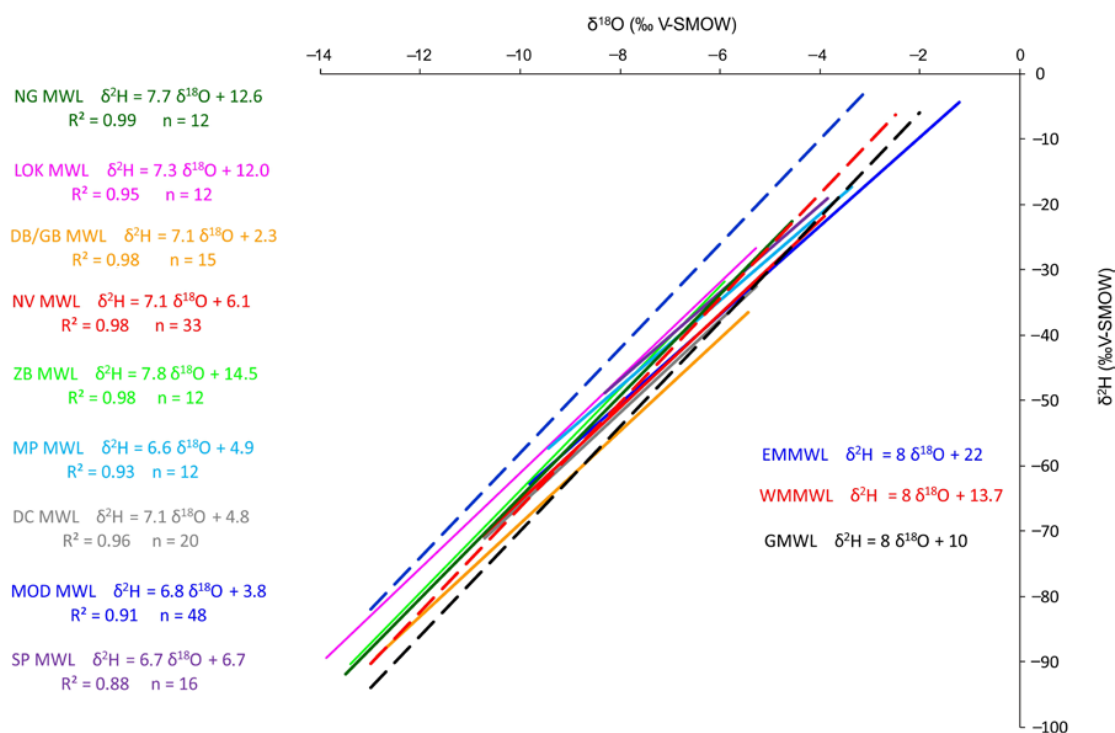


**Figure 4.** Local meteoric water lines (LMWL) of nine studied locations (NG, LOK, GB/DB, NV, ZB, MP, DC, MOD, SP) plotted alongside global (GMWL:  $\delta^2\text{H} = 8 \times \delta^{18}\text{O} + 10$  [66]), eastern Mediterranean (EMMWL:  $\delta^2\text{H} = 8 \times \delta^{18}\text{O} + 22$  [64]), and western Mediterranean meteoric water line (WMMWL:  $\delta^2\text{H} = 8 \times \delta^{18}\text{O} + 13.7$  [67]) – dashed lines. NV relates to ‘North Velebit’, as the rainwater was collected at three locations in VEL, SIR and LUK caves’ vicinity. For clarity, single-sample data points are removed, but they are visible in Figures 5–7 for each particular LMWL. Equations are sorted by the latitude of the site.

#### 4.2. Precipitation-Discharge Relationship and Drip Water Homogenization

When reconstructing multi-annual environmental changes using slow-growing stalagmites, one of the first issues to consider when interpreting particular drip water isotopic signals is the homogenization of the meteoric water during its transition through the epikarst towards the drip site, to ensure that the recorded speleothem  $\delta^{18}\text{O}$  signal is not seasonally biased. Homogenization of the drip water, i.e., removal of the seasonal signal of precipitation, had been initially taken as a rule [69], but it has since been realized that it must be considered as a site-specific process which is not always achieved, sometimes not even within the same cave [9,25,70–72]. As presented in Table 2, seasonal variations of rainwater  $\delta^{18}\text{O}$  (amplitudes from 4.5‰ to 8.9‰) and  $\delta^2\text{H}$  (amplitudes from 27.4‰ to 68.9‰) show some geographical/climate related distribution, being smaller in southern and coastal regions, while the northern and continental sites receive precipitation with a wider isotopic range. On the other hand,

the smaller amplitude of drip water  $\delta^{18}\text{O}$  (from 0.3‰ to 2.1‰) and  $\delta^2\text{H}$  (from 1.0‰ to 18.3‰) shows significant attenuation of the seasonal rainwater signal, regardless of geographical position.

Groundwater homogenization strongly depends on karst aquifer architecture, which also plays an important role in controlling drip discharge dynamics [73]. Infiltration-discharge relationships were observed in six caves and drip intensities recorded in caves with multiple drip-loggers (NG, LOK, MP, MOD, SP), confirming heterogeneity of the karst aquifers and their typical triple porosity nature with: (i) slow diffuse matrix flow, (ii) fracture and fissure flow and (iii) fast preferential flow through solution-enhanced conduits [74,75]. Discharge with significant variability and coherency with surface rain events can tentatively point to the lower degree of homogenization, i.e., partially preserved seasonal signal, so drip water  $\delta^{18}\text{O}$ - $\delta^2\text{H}$  pairs plotted in  $\delta^{18}\text{O}$ - $\delta^2\text{H}$  space appear scattered along the precipitation regression line. For example, according to concurrent daily rainfall totals and drip-logger records, MP-1 and MP-3 (Figure 5) demonstrated fast responses to surface rain events through epikarst fissures [25]. Similarly, MOD-22 also showed some seasonal variability (Figure 5), but is strongly out of phase with rainfall values, with the highest values during the winter. Apparently, this is a consequence of ‘piston-flow’ when newly recharged rainwater pushes through previously stored and partly mixed water [37]. On the other hand, densely clustered drip water values like those of MOD-31 and MOD-32 (Figure 5) coincide with very stable discharge regimes, practically unresponsive both to droughts and massive rain events [25]. Still, the peculiarity of karst systems is evident in LOK and NG caves. Drip sites LOK-1 and LOK-2 show evidence of typical fracture-flow or ‘seasonal drip’ regimes according to the classification by Smart and Friederich [76] and Baker et al., [58], with practically identical drip records [25]. However, LOK-1 preserves an attenuated seasonal signal which is completely dampened in LOK-2 (Figure 6). The opposite situation is observed in NG cave; drip water isotopic compositions of NG-2 and NG-3 are almost the same with minimal amplitudes (Figure 6) in spite of substantially different hydrological behaviour. NG-3, with typical matrix porosity, sustains stable discharge throughout the year, while NG-2 probably has a more complex route that includes ‘overflow’ storage reservoirs [3] expressed as fast response to major rain events and subsequent long-term decrease in discharge [25].

**Table 3.** Amount-weighted annual mean of precipitation and drip water  $\delta^{18}\text{O}$ ,  $\delta^2\text{H}$  and  $d$ -excess. For the drip sites not equipped with drip loggers, only average ( $\pm 1\sigma$ ) values are given. Sites are arranged by latitude. All the values are given in ‰ with respect to VSMOW.

Cave	$\delta^{18}\text{O}_{\text{prec}}$	$\delta^2\text{H}_{\text{prec}}$	$\delta^{18}\text{O}_{\text{drip}}$	$\delta^2\text{H}_{\text{drip}}$	$\Delta\delta^{18}\text{O}_{\text{prec-drip}}$	$\Delta\delta^2\text{H}_{\text{prec-drip}}$	$d$ -excess-Prec.	$d$ -excess-Drip
NG	−9.1	−57.1	−9.8 −9.8	−64.3 −63.5	0.7 0.7	7.2 6.4	15.6	14.3 14.9
LOK	−8.8	−51.8	−8.9 −8.6	−52.8 −50.9	0.1 −0.2	1.0 −0.9	18.6	18.5 18.0
GB-DB	−9.5	−64.9	−10.7 ± 0.3 −10.6 ± 0.2 −10.3 ± 0.5 −10.7 ± 0.5	−73.7 ± 2.1 −72.7 ± 0.7 −70.2 ± 3.0 −73.7 ± 3.5	1.2 ± 0.3 1.1 ± 0.2 0.8 ± 0.5 1.2 ± 0.5	8.8 ± 2.1 7.8 ± 0.7 5.3 ± 3.0 8.8 ± 3.5	11.0	12.0
VEL-S <sup>1</sup>	−9.5	−61.9			0.1 ± 0.1	0.0 ± 0.7	13.7	
VEL-O <sup>2</sup>	−9.4	−60.9	−9.6 ± 0.1 <sup>3</sup>	−61.9 ± 0.7 <sup>3</sup>	0.2 ± 0.1	1.0 ± 0.7	13.1	15.0 ± 0.5
ZB	−9.9	−62.2	−7.8 ± 0.3	−44.6 ± 2.5	−1.2 ± 0.3	−17.6 ± 2.5	16.6	16.3 ± 0.6
MP	−7.5	−44.3	−7.3	−42.0	−0.2	−2.3	15.5	16.2
DC	−8.6–−7.5 <sup>4</sup>	−56.5–−48.1 <sup>4</sup>	−8.0 ± 0.3	−49.0 ± 1.7	−0.6–0.5	−7.5–0.9	12.0–13.0	15.0
MOD	−5.5	−33.3	−6.0 −6.1	−36.5 −37.2	0.5 0.6	3.2 3.9	10.3	11.3 11.8
SP	−6.7	−38.3	−6.5	−34.4	−0.2	−3.9	15.2	17.3

<sup>1</sup> precipitation collected at location Siča; <sup>2</sup> precipitation collected at location Oltari; <sup>3</sup> cave water was collected only during five days of caving in August 2012; <sup>4</sup> different values depending on the considered period.

### 4.3. Isotopic Composition of Drip Water

The relationship between rain and drip water  $\delta^2\text{H}$ - $\delta^{18}\text{O}$  pairs of coastal and insular sites is shown in Figure 5. MOD, MP and SP caves are presented by at least one-year series of rain and drip water monthly—integrated samples and associated LMWLs, while MED, VRD, KRA, VML and MML are represented by data from one–two drip water samples. Just the latter are plotted, and further analyses of these sites are unfeasible without extended monitoring. When compared to continental sites, the series from MP, SP and 2008–2010 MOD rainwater data have a relatively narrow range (Table 2) due to the moderate maritime effect on temperature [68], with the exception of the longest MOD data set (2014–2018) which encompasses several extreme meteorological events with the most anomalous values. The similarity of LMWL slopes points to the same water vapor sources and infiltration conditions, but the aquifer architecture subsequently assumes the lead role. In the case of MOD cave, we can distinguish three different drip regimes and corresponding isotopic compositions (Table 2); MOD-21W and MOD-22W had lower and higher variability, respectively, while MOD-31W and MOD-32W are characterized by strong drip water homogenization [25]. Therefore, we took these sites as representative since that is the preferable hydrologic behavior for the best climate record in speleothems. The amount-weighted annual mean of precipitation  $\delta^{18}\text{O}$  is 0.5–0.6‰ higher than the amount-weighted annual mean of drip water  $\delta^{18}\text{O}$  (Table 3), meaning that effective infiltration and accumulation within aquifer occurs during the winter period. As for MP and SP caves, they both had amount-weighted annual means of precipitation  $\delta^{18}\text{O}$  0.2‰ lower in comparison to that of drip water (Table 3). These caves are very geographically different, insular SP at 70 m a.s.l. and mountain MP at 570 m a.s.l., but they have similar morphologies, i.e., descending chambers which maintain significantly lower temperatures. In SP cave, the MAAT is 11.1 °C, while surface MAAT is 16.4 °C, and in the case of MP, cave MAAT is 9.0 °C and surface MAAT is 13.7 °C [35]. This difference of  $5.0 \pm 0.3$  °C complicates the classification of these caves in terms of climatic controls on the isotopic composition of drip water as discussed in Baker et al. [77].

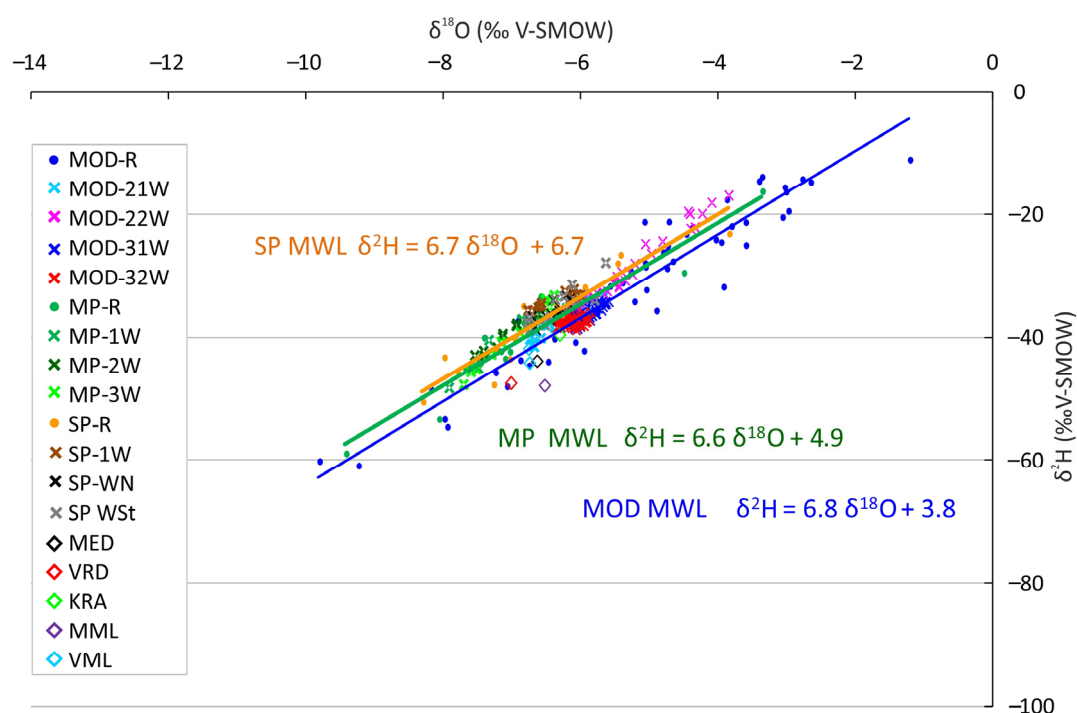


**Figure 5.**  $\delta^2\text{H}$ - $\delta^{18}\text{O}$  relationship of monthly integrated drip water (crosses) and rainwater samples (dots) with associated local meteoric waterlines in SP, MP and MOD caves, and of single drip water samples from low-altitude coastal caves MED, VRD, KRA, VML and MML (diamonds).

The relationship between precipitation and drip water isotopic composition of continental sites NG, LOK, GB, DB and DC is given in Figure 6.  $\delta^2\text{H}$  and  $\delta^{18}\text{O}$  have wide ranges due to the strong seasonal temperature variations [68], among which DC's smallest amplitude (Table 2) reflects its southernmost position (Figure 1). Drip water isotopic values of NG, GB and DB sites suggest larger contributions of winter precipitation, with a difference between amount-weighted annual mean precipitation and average drip water  $\delta^{18}\text{O}$  of 0.7‰ in NG cave, 0.8–1.2‰ in GB and 1.1–1.2‰ in DB cave (Table 3), at least for the monitoring period [36]. Caves with lower temperatures (LOK and DC) showed a different pattern; their drip water mean  $\delta^{18}\text{O}$  values were distributed around the amount-weighted annual mean of precipitation  $\delta^{18}\text{O}$  (Table 3), with indistinguishable preferential recharge period.

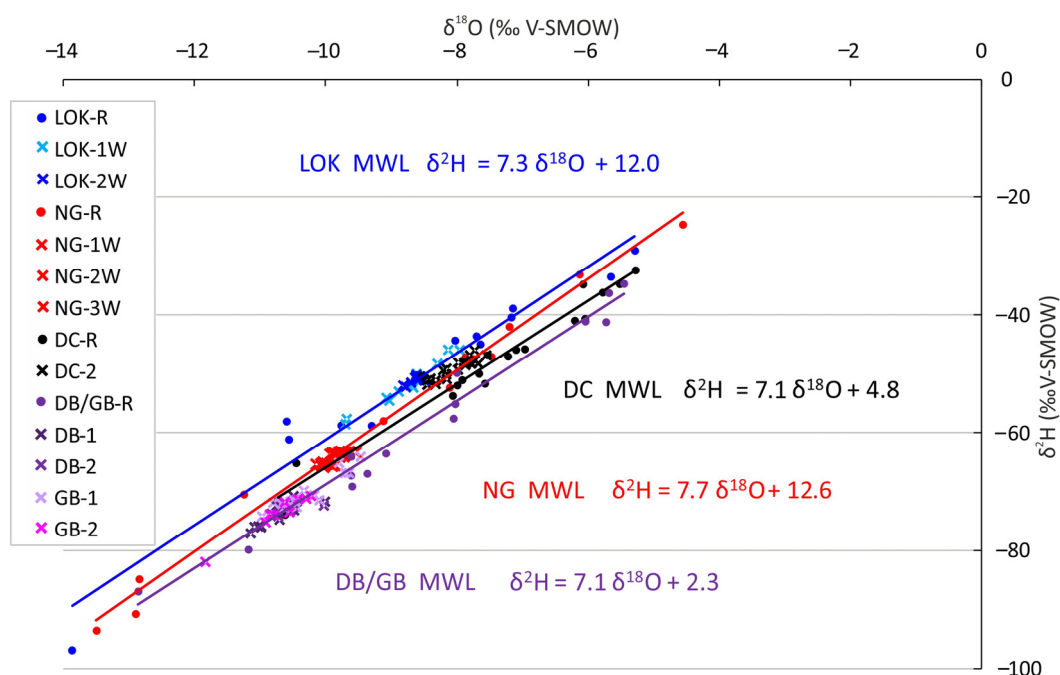


**Figure 6.**  $\delta^2\text{H}$ - $\delta^{18}\text{O}$  relationship of monthly integrated drip water (crosses) and rainwater samples (dots) with associated local meteoric waterlines in mid-altitude continental caves NG, LOK, DB, GB, DC.

The hydrology of the high-mountain caves is represented by two LMWLs (Figure 7). North Velebit caves (VEL, LUK, SIR) located at 1450–1550 m a.s.l. are in fact vertical shafts; LUK and SIR caves are characterized by perennial snow and ice accumulation in the upper portions [49–51,78], while VEL cave is ice-free due to its morphology, i.e., horizontal entrances [49]. According to the drip water samples from VEL cave, these aquifers are predominantly fed by September–May precipitation [39]. Average annual duration of snow cover ( $\geq 1$  cm) in that region is 165 days (Zavižan station 1981–2010, CMHS, 2020) and most of the recharge is meltwater, hence the grouping of drip water  $\delta^2\text{H}$ - $\delta^{18}\text{O}$  data along the lowermost part of the NV MWL (Figure 7). The difference between the amount-weighted annual mean precipitation and average drip water  $\delta^{18}\text{O}$  is 0.1–0.2‰ (Table 3, Figure 8), although Figure 7 would suggest a larger difference.

ZB cave is at a lower altitude (1250 m a.s.l.) and is not an ice cave; snow cover lasts considerably shorter than in the North Velebit sites. Its LMWL clearly shows partly evaporative conditions at the water-vapor source and minimal secondary evaporation during precipitation (Figure 7), consistent with its geographic location. Drip water was relatively uniformly discharged and homogenized [35]. However, the isotopic composition demonstrates significant departure towards the summer values (Figure 7), so the amount-weighted annual mean of precipitation  $\delta^{18}\text{O}$  was  $1.2 \pm 0.3$ ‰ lower than the annual mean of drip water  $\delta^{18}\text{O}$ .

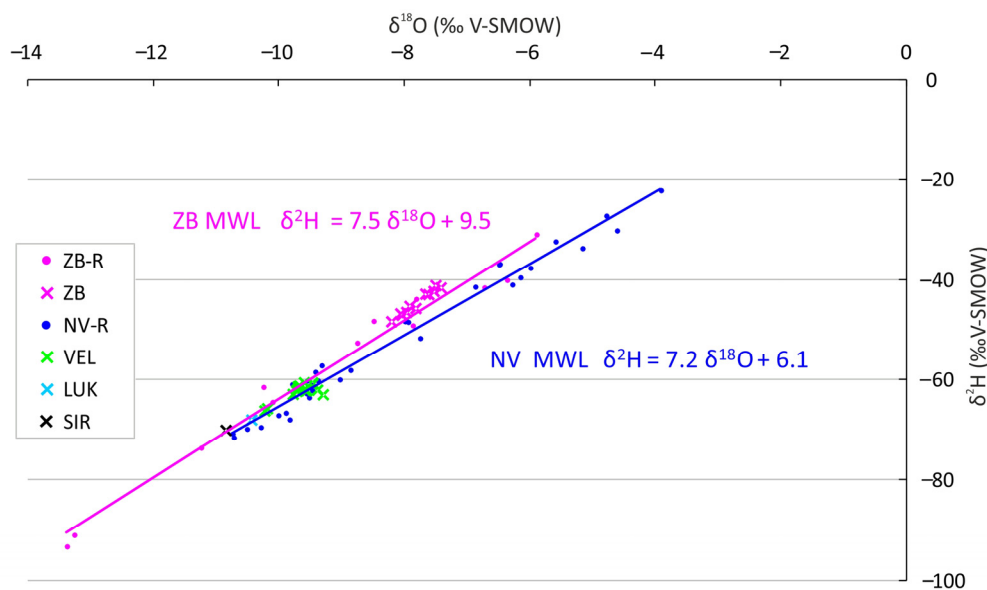


**Figure 7.**  $\delta^2\text{H}$ - $\delta^{18}\text{O}$  relationship of monthly integrated drip water (crosses) and rainwater samples (dots) with associated local meteoric water lines in high-altitude mountain—caves ZB, VEL, SIR, LUK. NV relates to ‘North Velebit’, as the rainwater was collected at three locations in VEL, SIR and LUK caves vicinity.

Recently, Baker et al., [77] conducted a global analysis of rain and drip water data from 39 caves on five continents and demonstrated that the extent to which drip water  $\delta^{18}\text{O}$  is representative of amount-weighted precipitation  $\delta^{18}\text{O}$  is related to MAAT and annual precipitation, which determines the extent to which the isotopic signal is additionally altered by soil and karst processes. It was concluded that caves with a MAAT  $<10^\circ\text{C}$  show minimal differences between drip water  $\delta^{18}\text{O}$  and amount-weighted precipitation  $\delta^{18}\text{O}$ ; Croatian ‘cold’ caves LUK, VEL, SIR, DC and LOK generally fit into that classification (Figure 9), i.e., their  $\Delta\delta^{18}\text{O}_{\text{prec-drip}}$  vary around 0‰. The peculiar exception is ZB cave with a large drip water  $\delta^{18}\text{O}$  departure towards summer values ( $\Delta\delta^{18}\text{O}_{\text{prec-drip}} = -1.2 \pm 0.3\text{‰}$ ) (Figure 8). Given the relatively uniform discharge (checked by manual drip counting during each visit [35]) and homogenized drip water (attenuation of rainfall  $\delta^{18}\text{O}$  amplitude of 7.5‰ to the drip water  $\delta^{18}\text{O}$  range 0.8‰, Table 3) it is apparent that the isotopic signal of any individual recharge events is buffered, giving the credible drip water average. Such a significant  $\delta^{18}\text{O}$  increase may be ascribed to evaporative fractionation, which is quite unrealistic in a high-mountain region with a MAAT of  $4.0^\circ\text{C}$ , but on the other hand the constant in-cave atmospheric conditions in ZB has been occasionally disturbed and RH has decreased during dry bora wind episodes [35].

Other studied Croatian regions would fit into the class with MAAT between  $10^\circ\text{C}$  and  $16^\circ\text{C}$  (we included here also MOD region with MAAT  $16.6^\circ\text{C}$ , as a marginal case) in which the drip water  $\delta^{18}\text{O}$  may be affected by evaporative fractionation of the water in the soil and epikarst or by selective recharge, resulting in  $|\Delta\delta^{18}\text{O}_{\text{prec-drip}}| > 0.3\text{‰}$  [77]. Such values are recorded in MOD, NG, DB and GB caves, but not in the two littoral caves, MP and SP, which are characterized with  $|\Delta\delta^{18}\text{O}_{\text{prec-drip}}| < 0.3\text{‰}$ , as if they were ‘cold’ caves. In particular, the amount-weighted annual means of precipitation  $\delta^{18}\text{O}$  are lower by 0.2‰ in comparison to that of drip waters which is a consequence of the combined influence: of (i) evaporative fractionation due to relatively high MAAT and especially summer temperatures; (ii) selective recharge during the autumn and winter seasons; and (iii) the decrease of cave MAAT in relation to surface MAAT by  $5.0 \pm 0.3^\circ\text{C}$ .

Apart from the occasionally necessary drip-specific interpretation, and morphologically driven exceptions, it must be considered that during glacial periods, today’s ‘warm’ caves assumed cold-cave characteristics. Thus, within a single speleothem which covers one or more glacial-interglacial shifts, different climate control on  $\Delta\delta^{18}\text{O}_{\text{prec-drip}}$  would be experienced [77].

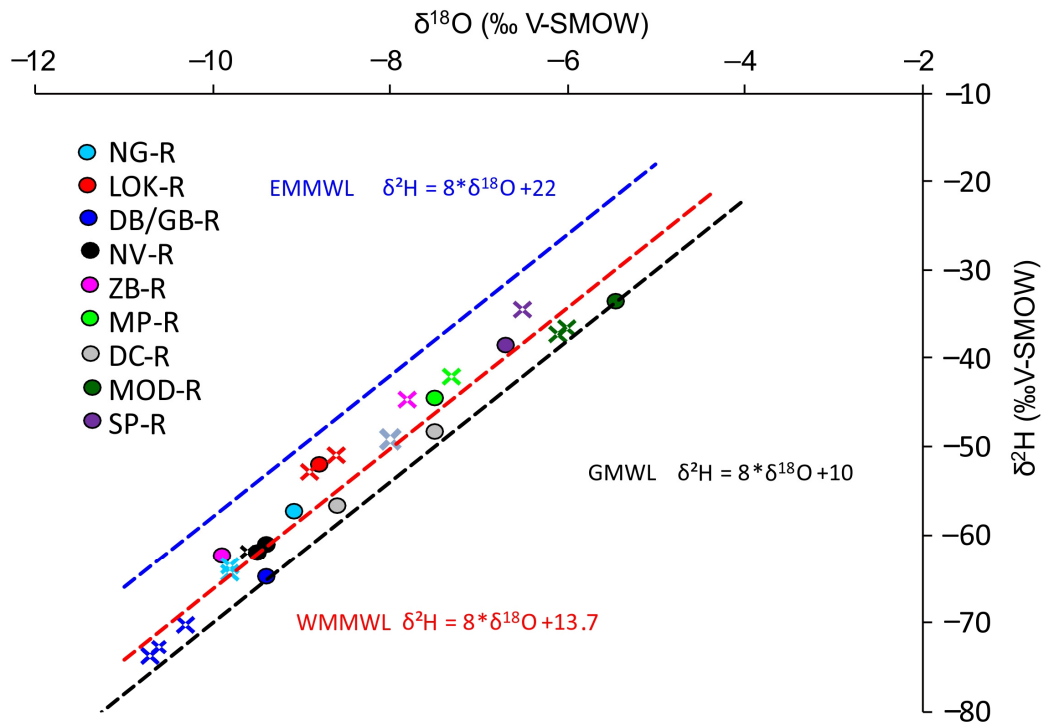


**Figure 8.** Amount-weighted annual mean of precipitation (circles) and drip water  $\delta^{18}\text{O}$  and  $\delta^2\text{H}$  (crosses) in relation to the global (GMWL:  $\delta^2\text{H} = 8 \times \delta^{18}\text{O} + 10$  [66]), eastern Mediterranean (EMMWL:  $\delta^2\text{H} = 8 \times \delta^{18}\text{O} + 22$  [64]), and western Mediterranean meteoric water line (WMMWL:  $\delta^2\text{H} = 8 \times \delta^{18}\text{O} + 13.7$  [67]). The LUK-VEL-SRI values represent precipitation collected at two neighboring sites (Siča and Oltari [39]) during 2012–2013 for 17 months, but with several gaps, so only tentative values are given (calculated as averages of several different intervals). For the unlogged drip sites (ZB, GB, DB, DC), we used annual averages instead of amount-weighted  $\delta^{18}\text{O}$  and  $\delta^2\text{H}$  values. Sites are arranged by latitude in the legend box.

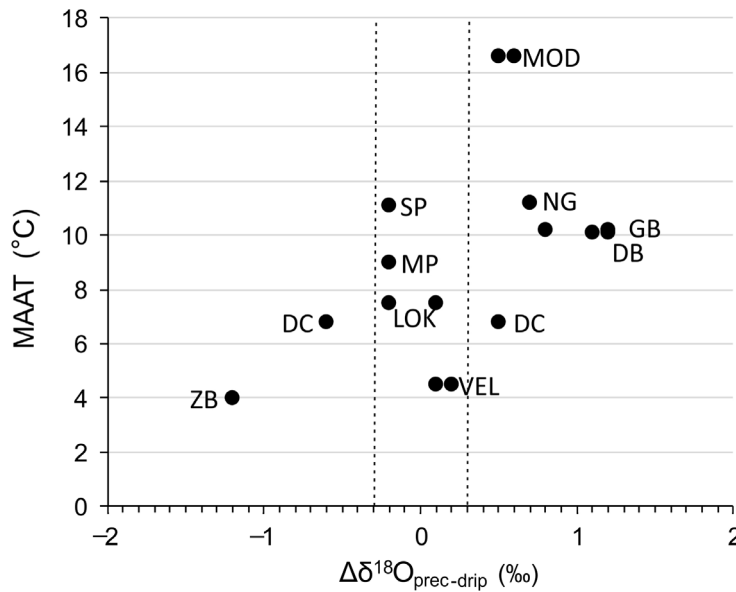


**Figure 9.** Relationship between  $\Delta\delta^{18}\text{O}_{\text{prec-drip}}$  and mean annual air temperature (MAAT). Vertical lines show the 0.3‰ criterion for determining the significant difference between amount-weighted annual means of precipitation  $\delta^{18}\text{O}$  and drip water  $\delta^{18}\text{O}$  [77].

#### 4.4. Preservation of Altitude and Latitude Effects in Drip Water

Due to the upward deflection by the mountain barrier, air masses decompress and cool adiabatically, so the rainout is enhanced [79], and due to the temperature decrease with elevation, the 'altitude effect' is characterized by a decrease in  $\delta^{18}\text{O}$  values. When considering precipitation, an average gradient ( $\Delta\delta^{18}\text{O}/100\text{ m}$ ) of  $-0.2\text{‰}$  is estimated globally [80], but since topography strongly influences isotopic composition, especially if the relief is high [79], local gradients are even higher. When comparing precipitation and drip water isotopic composition, infiltration elevation must be taken into account since the altitude of the catchment area can be substantially higher than the elevation of the drip water collection site, delivering more depleted water. Our observed profile extends from MOD cave at 32 m a.s.l. via MP cave (570 m a.s.l.) to ZB at 1250 m a.s.l. across a horizontal distance of 13.6 km, and according to the amount-weighted mean annual precipitation  $\delta^{18}\text{O}$  ( $-5.5\text{‰}$ ,  $-7.5\text{‰}$  and  $-9.9\text{‰}$ , respectively), the local  $\Delta\delta^{18}\text{O}/100\text{ m}$  gradient is  $-0.36\text{‰}$  (Figure 10). As for the infiltration elevation of these three caves, their recharge areas are limited by relatively thin overburden and positions near the summits, so drip water does not carry a depleted isotopic signal from much higher elevations. The observed drip water  $\Delta\delta^{18}\text{O}/100\text{ m}$  gradient is  $-0.15\text{‰}$  (Figure 10), comparable to steep north Italian Alps where two transects had gradient of  $-0.15\text{‰}$  and  $-0.08\text{‰}$  [81]. It is also similar to a steep coastal area on Vancouver Island where the drip water gradient was  $-0.16\text{‰}$  [72] and the western flank of Mount-Lebanon where it was  $-0.2\text{‰}$  [82]. However, MP and ZB sites, as mentioned above, may not be the best representatives for general conclusions on the altitudinal effect on drip water due to their specific settings, but it is indicative that the drip water gradient is attenuated according to precipitation gradient.

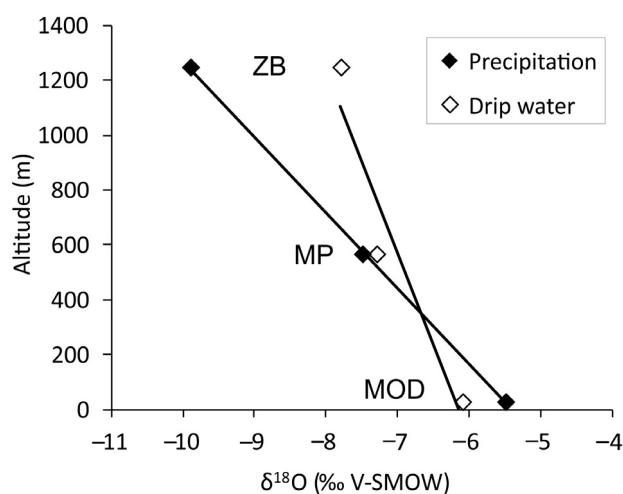


**Figure 10.** Comparison of altitudinal gradient in precipitation and drip water on steep Mt Velebit seaward slope based on MOD (32 m a.s.l.), MP (570 m a.s.l.) and ZB (1250 m a.s.l.) site values  $\delta^{18}\text{O}$ .

The latitude effect on precipitation  $\delta^{18}\text{O}$  in mid-latitude regions is about  $-0.5\text{‰}$   $\delta^{18}\text{O}$  per degree of latitude [77]. In the studied Croatian sites, the gradient is apparent (Figure 8), but the absolute value is undetectable as it is partly overprinted by the altitude effect. The same situation is evident in the drip waters.

#### 4.5. Isotope Fractionation during Carbonate Formation

Based on the previous sections, it is evident that the drip water and its stable isotope composition have great significance in preserving and inheriting climatic information that can be transferred to the speleothem. However, this preservation strongly depends on the fraction which took place during the carbonate formation. Therefore, it is essential to establish the equation which describes the isotope fraction during the speleothem formation (i.e., carbonate precipitation) at each cave site.



The stable isotope composition of modern calcite and concomitant drip water together with the cave air temperature can be utilized to select the equations which best express isotope fractionation. Among the caves reviewed in this study, modern carbonate precipitates were collected at MOD, MP, DB, GB and SP and the related data are summarized in Table 4.

**Table 4.** Oxygen isotope composition of modern calcite and concomitant drip water and measured ( $T_m$ ) and calculated ( $T_c$ ) cave air temperature.  $T_c$  values closer to the  $T_m$  are emboldened. Note that for calculations, the  $\delta^{18}O_{\text{calcite}}$  value was converted from VPDB (Vienna Pee Dee Belemnite) to VSMOW using the expression  $\delta^{18}O_{\text{VSMOW}} = 1.03091 \times \delta^{18}O_{\text{VPDB}} + 30.91$  [83]. Temperatures are calculated according to Tremaine et al., [84] and Daëron et al., [85]. The uncertainties of the  $\delta^{18}O$  analyses (both for calcite and water) is generally 0.1‰ (see Appendix A).

Cave	Sample ID	$\delta^{18}O_{\text{calcite}}$ (‰ VPDB)	$\delta^{18}O_{\text{drip water}}$ (‰ VSMOW)	$T_m$ (°C)	$T_c$ (°C) Tremaine et al. (2011)	$T_c$ (°C) Daëron et al. (2019)
MOD	MOD 8	−5.5	−5.8	15.6	<b>17.7</b>	19.4
	MOD 9	−5.3	−5.8	15.6	<b>16.5</b>	18.3
MP	MPC3	−5.4	−7.2	9.2	<b>9.8</b>	12.1
	MPC4	−5.5	−7.2	9.2	<b>10.4</b>	12.6
	MPC5	−5.4	−7.2	9.2	<b>10.1</b>	12.3
	MPC6	−5.2	−7.2	9.2	<b>9.1</b>	11.5
SP	SPC2	−4.3	−6.6	11.1	7.5	<b>9.9</b>
	SPC3	−4.4	−6.6	11.1	8.2	<b>10.5</b>
	SP1WC	−5.0	−6.6	10.3	<b>11.0</b>	13.2
	SP1WC	−4.7	−6.8	10.6	8.3	<b>10.7</b>
	SPNC	−4.8	−6.5	10.3	<b>10.6</b>	12.8
DB	DB1	−8.1	−10.7	9.9	6.2	<b>8.7</b>
	DB2	−8.9	−10.6	11.1	10.5	<b>12.7</b>
GB	GB1	−8.7	−10.3	9.7	<b>10.9</b>	13.1
	GB2	−8.4	−10.7	10.9	7.6	<b>10.1</b>

In Figure 11 the calculated values are plotted along with equations based on theoretical, experimental and empirical investigations [11,84–87]. Most of the data are scattering along the equations line obtained from empirical observation by Tremaine et al. [84] ( $1000\ln\alpha = 16.1 \times 10^3/T - 24.6$ ), and Daëron et al. [86] ( $1000\ln\alpha = 17.57 \times 10^3/T - 29.13$ ); the latter is almost identical to the equation determined by Coplen (2007). Therefore, utilizing these equations and the measured stable isotope composition, the temperature can be calculated ( $T_c$ ) and compared with those observed in the cave ( $T_m$ ). There are also some data (e.g., MOD) which plot between equations by Tremaine et al., [84] and Friedmann and O’Neil [86] ( $1000\ln\alpha = 2.78 \times 10^6/T^2 - 2.89$ ). Interestingly, even in the same cave system (e.g., DB/GB, SP) distinct isotope fraction can take place, drawing attention to the importance of studying in-situ calcite precipitation for all sites from where speleothems are taken for investigation in order to reconstruct past climate and environmental changes [36].

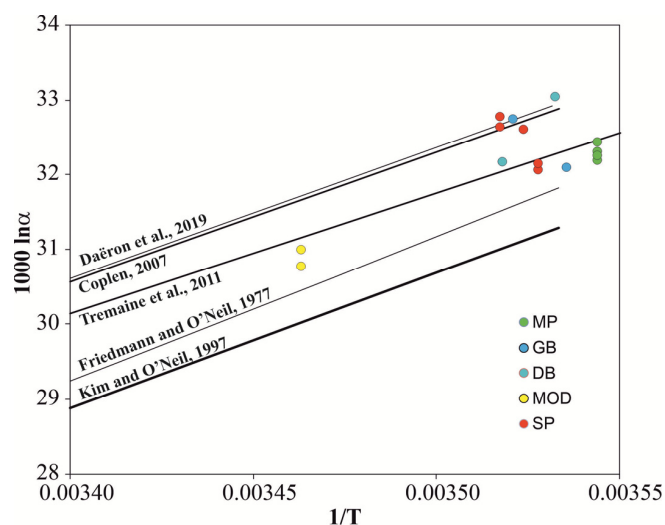


**Figure 11.** Calcite-water  $1000 \ln \alpha$  values vs.  $1/T$  (in K) measured for modern carbonates samples from MP, DB, GB, MOD and SP caves and selected published curves [11,84–87]. Calcite/water fractionation factor  $\alpha = (1000 + \delta^{18}\text{O}_{\text{calcite}})/(1000 + \delta^{18}\text{O}_{\text{water}})$ .

## 5. Conclusions

We revisited the stable isotope composition of precipitation and drip water from 17 Croatian caves with the intention of characterizing the main features essential for interpretation of speleothem isotope records in local and regional paleoenvironmental studies. To summarize:

- Nine constructed local meteoric water lines generally show influence of both Atlantic and Western Mediterranean vapor masses, and individually clearly depict particular regions with enhanced secondary evaporation.
- Drip waters in mountain and continental caves with MAAT < 10 °C drip water  $\delta^{18}\text{O}$  mostly resemble the amount-weighted annual mean  $\delta^{18}\text{O}$  of precipitation. These are the caves where the soil and epikarst evaporation has decreased, and groundwater is well mixed with a dampening of individual extreme events. Thus, in near-equilibrium calcite crystallization, speleothem  $\delta^{18}\text{O}$  variations most faithfully reflect past meteoric precipitation and air temperature.
- In warmer caves, drip water  $\delta^{18}\text{O}$  is usually more negative than amount-weighted annual mean precipitation  $\delta^{18}\text{O}$  due to the uneven seasonal recharge and near-surface evaporation. However, when interpreting the interglacial-glacial transition it must be taken into consideration that MAATs have decreased to those of today's 'cold' caves and the isotopic signal probably directly reflects recharge.
- The precipitation altitude effect on seaward steep coastal mountains is higher than globally estimated, enhanced by sudden change from Mediterranean climate (Csa and Csb) to mountain (Df) climate. In drip water, the altitudinal gradient is also present, but less expressed.
- The latitude effect in drip water is present, but often overprinted by the altitudinal effect.

Among all derived conclusions, this is the first and foremost guiding principle against which all actions need to be conducted in forthcoming studies.

- This spatially small, but geographically very diverse area does not allow generalization; frequent exceptions of anticipated settings require thorough monitoring of surface and cave meteorological background since cave morphology (ascending/descending passages) may alter the cave temperature from those equal to the surface MAAT. Systematic analyses of drip water geochemistry may also reveal potentially different infiltration elevations, while monitoring of drip intensity provides information on aquifer architecture responsible for the water homogenization. Preferably, all of these steps should precede speleothem collection in order to avoid their oversampling.

**Author Contributions:** Conceptualization, methodology and investigation, M.S., R.L., N.L., G.C. and N.B.; formal analysis, R.N.D. and P.B.; visualization, M.S., N.B., R.L. and G.C.; writing—original draft preparation, M.S., R.L. and G.C.; writing—review and editing, M.S., G.C., R.L., N.B., P.B. and R.N.D. All authors have read and agreed to the published version of the manuscript.

**Funding:** This research received no external funding. Data have been obtained during the projects *Reconstruction of the regional paleoclimate change—speleothem records from the North Dalmatia (Croatia)* (60200) funded by the University of Zadar, *Reconstruction of the Quaternary environment in Croatia using isotope methods* (HRZZ-IP-2013-11-1623) funded by the Croatian Science Foundation, and *Research of geomorphological-geological conditions of karst and hydro-morphological peculiarities on selected localities of the Dinaric karst in Croatia* (20284703) funded by the University of Zagreb. N.L. was granted with Unity Trough Knowledge Fund Grant (71/10) and G. C. was granted by Hungarian Scientific Research Fund (PD 121387) and János Bolyai Research Scholarship of the Hungarian Academy of Sciences.

**Acknowledgments:** Meteorological data were obtained on request (free of charge) from the Croatian Meteorological and Hydrological Service. Two anonymous reviewers and Guest Editor are gratefully acknowledged for the constructive suggestions that improved the manuscript.

**Conflicts of Interest:** The authors declare no conflict of interest. The funders had no role in the design of the study; in the collection, analyses, or interpretation of data; in the writing of the manuscript, or in the decision to publish the results.

## Appendix A

Stable isotope composition of rain and drip water from NG, LOK, ZB, MP, SP and MOD (2014–2018) was carried out on ~2 mL subsamples of filtered sample water using a Picarro L2120 cavity ring-down isotope analyzer at the School of Geography, The University of Melbourne. Sample isotopic ratios were normalized to the international VSMOW scale using a four point calibration using two international (GISP2, VSMOW) and two in-house standards (WOOLIES, LAKE) of known composition. The results from the WOOLIES standards were used to determine the analytical uncertainty ( $1\sigma$ ) which was  $\leq 0.1\text{‰}$  for  $\delta^{18}\text{O}$  and  $\leq 0.3\text{‰}$  for  $\delta^2\text{H}$  for MP, SP and ZB samples and  $0.05\text{‰}$  for  $\delta^{18}\text{O}$  and  $0.13\text{‰}$  for  $\delta^2\text{H}$  for NG, LOK and MOD (2014–2018) samples. Samples were re-analyzed in cases where the uncertainty on the three injections lay outside  $0.1\text{‰}$  for  $\delta^{18}\text{O}$  and  $\leq 0.3\text{‰}$  for  $\delta^2\text{H}$ .

Oxygen and hydrogen isotope measurements on the MOD water samples in 2008–2010 were carried out at SILLA (Stable Isotope & Luminescence Laboratory) at the University of Birmingham, UK, while the MOD water samples in 2007–2008 campaign were analyzed by Thermo-Finnigan DELTAplusXP isotope ratio mass spectrometer, fitted with a gas bench and an autosampler at SILab Rijeka (Stable Isotope Laboratory at the Physics Department, School of Medicine, University of Rijeka). Results were normalized using VSMOW-calibrated SILab in-house standards (DZW, RTW, MGS and AAS reported in Mandić et al., [88]) and analytical reproducibility in dual inlet measurements were better than  $0.1\text{‰}$  for  $\delta^{18}\text{O}$  and  $1\text{‰}$  for  $\delta^2\text{H}$ . The same facilities were used for the water analyses on SIR, LUK and VEL samples, with the same measurement precision [39].

Stable isotope analyses of the water samples from GB, DB and DC caves were performed at the Institute for Geological and Geochemical Research (IGGR) in Budapest, Hungary, using a Liquid-Water Isotope Analyser-24d manufactured by Los Gatos Research. The instrument uses off-axis integrated cavity ring down spectroscopy to measure the absolute abundances of  $^2\text{H}^1\text{H}^{16}\text{O}$ ,  $^1\text{H}^1\text{H}^{18}\text{O}$  and  $^1\text{H}^1\text{H}^{16}\text{O}$  via laser absorption. Measured isotopic ratios were normalized to the homemade laboratory standards, which were calibrated to international standards ( $\delta^{18}\text{O} = -0.53\text{‰}$ ;  $-10.41\text{‰}$ ;  $-19.95\text{‰}$ ;  $\delta^2\text{H} = -9.0\text{‰}$ ;  $-74.9\text{‰}$ ;  $-147.7\text{‰}$  for BWS1, BWS2, BWS3, respectively [89]. The precisions were better than  $0.15\text{‰}$  and  $1.0\text{‰}$  for  $\delta^{18}\text{O}$  and  $\delta^2\text{H}$ , respectively.

Water samples from MED, KRA, VRD, VML and MML caves were measured at the Geological Survey of Israel (GSI). Hydrogen isotope composition was measured by Thermo-Finnigan HighTemperature Conversion Elemental Analyzer (TC/EA) attached to a Delta V Thermo-Finnigan mass spectrometer and oxygen isotope composition was measured by Thermo-Finnigan GasBenchII attached to a Delta Plus mass spectrometer. The precision of these measurements was  $\pm 0.1\text{‰}$  for  $\delta^{18}\text{O}$  and  $\pm 1.5\text{‰}$  for  $\delta^2\text{H}$ .

Modern calcite from MP and SP caves i.e., carbon and oxygen stable isotope composition was analyzed using an Analytical Precision AP2003 continuous-flow isotope-ratio mass spectrometer at the School of Geography, The University of Melbourne, using the procedure described in

Drysdale et al., [90]. Sample results were normalized to the V–PDB scale using an in-house standard of Carrara Marble (NEW1) previously calibrated against the international standards, NBS18 ( $\delta^{13}\text{C} = 5.01\text{‰}$ ;  $\delta^{18}\text{O} = -23.01\text{‰}$ ) and NBS19 ( $\delta^{13}\text{C} = 1.95\text{‰}$ ;  $\delta^{18}\text{O} = -2.20\text{‰}$ ). Analytical uncertainty was better than 0.1‰ for  $\delta^{18}\text{O}$  and 0.05‰ for  $\delta^{13}\text{C}$ . DB and GB modern calcite samples were analyzed using an automated GasBench II sample preparation device attached to a Thermo–Finnigan DELTAplusXP mass spectrometer at the IGGR in Budapest, Hungary. Precision was better than 0.1‰ for both  $\delta^{18}\text{O}$  and  $\delta^{13}\text{C}$ . The same spectrometer was used for MOD (2008) modern calcite samples at SILab Rijeka and analytical reproducibility for both  $\delta^{18}\text{O}$  and  $\delta^{13}\text{C}$  was better than 0.1‰.

## References

1. Brantley, S.L.; Goldhaber, M.B.; Ragnarsdottir, K.V. Crossing Disciplines and Scales to Understand the Critical Zone. *Elements* **2007**, *3*, 307–314. [[CrossRef](#)]
2. Regattieri, E.; Zanchetta, G.; Isola, I.; Zanella, E.; Drysdale, R.N.; Hellstrom, J.C.; Zerboni, A.; Dallai, L.; Tema, E.; Lanci, L.; et al. Holocene Critical Zone dynamics in an Alpine catchment inferred from a speleothem multiproxy record: Disentangling climate and human influences. *Sci. Rep.* **2019**, *9*, 1–9. [[CrossRef](#)] [[PubMed](#)]
3. Fairchild, I.J.; Baker, A. *Speleothem Science: From Process to Past Environments*; Wiley-Blackwell: Chichester, UK, 2012.
4. Hendy, C.H.; Wilson, A.T. Palaeoclimatic Data from Speleothems. *Nature* **1968**, *219*, 48–51. [[CrossRef](#)]
5. Hendy, C.H. The Isotopic Geochemistry of Speleothems—I. The Calculation of the Effects of Different Modes of Formation on the Isotopic Composition of Speleothems and Their Applicability as Palaeoclimatic Indicators. *Geochim. Cosmochim. Acta* **1971**, *35*, 801–824. [[CrossRef](#)]
6. Henderson, G.M. CLIMATE: Caving In to New Chronologies. *Science* **2006**, *313*, 620–622. [[CrossRef](#)]
7. McDermott, F. Palaeo-Climature Reconstruction from Stable Isotope Variations in Speleothems: A Review. *Quat. Sci. Rev.* **2004**, *23*, 901–918. [[CrossRef](#)]
8. Badino, G. Models of temperature, entropy production and convective airflow in caves. *Geol. Soc. London Spec. Publ.* **2018**, *466*, 359–379. [[CrossRef](#)]
9. Baldini, J.; McDermott, F.; Fairchild, I.J. Spatial Variability in Cave Drip Water Hydrochemistry: Implications for Stalagmite Palaeoclimate Records. *Chem. Geol.* **2006**, *235*, 390–404. [[CrossRef](#)]
10. Fuller, L.; Baker, A.; Fairchild, I.J.; Spötl, C.; Marca-Bell, A.; Rowe, P.; Dennis, P.F. Isotope Hydrology of Dripwaters in a Scottish Cave and Implications for Stalagmite Palaeoclimate Research. *Hydrol. Earth Syst. Sci.* **2008**, *12*, 1065–1074. [[CrossRef](#)]
11. Kim, S.-T.; O’Neil, J.R. Equilibrium and nonequilibrium oxygen isotope effects in synthetic carbonates. *Geochim. Cosmochim. Acta* **1997**, *61*, 3461–3475. [[CrossRef](#)]
12. Hartmann, A.; Baker, A. Modelling Karst Vadose Zone Hydrology and Its Relevance for Palaeoclimate Reconstruction. *Earth Sci. Rev.* **2017**, *172*, 178–192. [[CrossRef](#)]
13. Banak, A.; Mandić, O.; Kovačić, M.; Pavelić, D. Late Pleistocene Climate History of the Baranja Loess Plateau—Evidence from the Zmajevac Loess-Paleosol Section (Northeastern Croatia). *Geol. Croat.* **2012**, *65*, 411–422. [[CrossRef](#)]
14. Wacha, L.; Galović, L.; Kolozár, L.; Magyar, Á.; Chikán, G.; Marsi, I. The Chronology of the Šarengrad II Loess-Palaeosol Section (Eastern Croatia). *Geol. Croat.* **2013**, *66*, 191–203. [[CrossRef](#)]
15. Wacha, L.; Rolf, C.; Hambach, U.; Frechen, M.; Galović, L.; Duchoslav, M. The Last Glacial Aeolian Record of the Island of Susak (Croatia) as Seen from a High-Resolution Grain-Size and Rock Magnetic Analysis. *Quat. Int.* **2018**, *494*, 211–224. [[CrossRef](#)]
16. Durn, G.; Rubinić, V.; Wacha, L.; Patekar, M.; Frechen, M.; Tsukamoto, S.; Tadej, N.; Husnjak, S. Polygenetic Soil Formation on Late Glacial Loess on the Susak Island Reflects Paleo-Environmental Changes in the Northern Adriatic Area. *Quat. Int.* **2018**, *494*, 236–247. [[CrossRef](#)]
17. Horvatinić, N.; Sironić, A.; Barešić, J.; Sonđi, I.; Krajcar Bronić, I.; Borković, D. Mineralogical, Organic and Isotopic Composition as Palaeoenvironmental Records in the Lake Sediments of Two Lakes, the Plitvice Lakes, Croatia. *Quat. Int.* **2018**, *494*, 300–313. [[CrossRef](#)]
18. Galović, I.; Mihalić, K.C.; Ilijanić, N.; Miko, S.; Hasan, O. Diatom Responses to Holocene Environmental Changes in a Karstic Lake Vrana in Dalmatia (Croatia). *Quat. Int.* **2018**, *494*, 167–179. [[CrossRef](#)]

19. Ilijanić, N.; Miko, S.; Hasan, O.; Bakrač, K. Holocene Environmental Record from Lake Sediments in the Bokanjačko Blato Karst Polje (Dalmatia, Croatia). *Quat. Int.* **2018**, *494*, 66–79. [[CrossRef](#)]
20. Bakrač, K.; Ilijanić, N.; Miko, S.; Hasan, O. Evidence of Sapropel S1 Formation from Holocene Lacustrine Sequences in Lake Vrana in Dalmatia (Croatia). *Quat. Int.* **2018**, *494*, 5–18. [[CrossRef](#)]
21. Felja, I.; Fontana, A.; Furlani, S.; Bajraktarević, Z.; Paradžik, A.; Topalović, E.; Rossato, S.; Ćosović, V.; Juračić, M. Environmental Changes in the Lower Mirna River Valley (Istria, Croatia) during Upper Holocene. *Geol. Croat.* **2015**, *68*. [[CrossRef](#)]
22. Kaniewski, D.; Marriner, N.; Morhange, C.; Rius, D.; Carre, M.-B.; Faivre, S.; Van Campo, E. Croatia's Mid-Late Holocene (5200–3200 BP) Coastal Vegetation Shaped by Human Societies. *Quat. Sci. Rev.* **2018**, *200*, 334–350. [[CrossRef](#)]
23. Brunović, D.; Miko, S.; Ilijanić, N.; Peh, Z.; Hasan, O.; Kolar, T.; Šparica Miko, M.; Razum, I. Holocene Foraminiferal and Geochemical Records in the Coastal Karst Dolines of Cres Island, Croatia. *Geol. Croat.* **2019**, *72*, 19–42. [[CrossRef](#)]
24. Faivre, S.; Bakran-Petricioli, T.; Barešić, J.; Horvatić, D.; Macario, K. Relative Sea-Level Change and Climate Change in the Northeastern Adriatic during the Last 1.5 Ka (Istria, Croatia). *Quat. Sci. Rev.* **2019**, *222*, 1–17. [[CrossRef](#)]
25. Surić, M. Speleothem-Based Quaternary Research in Croatian Karst—A Review. *Quat. Int.* **2018**, *490*, 113–122. [[CrossRef](#)]
26. Krajcar Bronić, I.; Horvatinčić, N.; Obelić, B. Two Decades of Environmental Isotope Records in Croatia: Reconstruction of the Past and Prediction of Future Levels. *Radiocarbon* **1998**, *40*, 399–416. [[CrossRef](#)]
27. Krajcar Bronić, I.; Vreča, P.; Horvatinčić, N.; Barešić, J.; Obelić, B. Distribution of hydrogen, oxygen and carbon isotopes in the atmosphere of Croatia and Slovenia. *Arch. Ind. Hyg. Toxicol.* **2006**, *57*, 23–29.
28. Krajcar Bronić, I.; Barešić, J.; Borković, D.; Sironić, A.; Mikelić, I.L.; Vreča, P. Long-Term Isotope Records of Precipitation in Zagreb, Croatia. *Water* **2020**, *12*, 226. [[CrossRef](#)]
29. Horvatinčić, N.; Krajcar Bronić, I.; Obelić, B.; Bistrotić, R. Long-time atmospheric tritium record in Croatia. *Acta Geol. Hung.* **1996**, *39*, 81–84.
30. Horvatinčić, N.; Krajcar Bronić, I.; Barešić, J.; Obelić, B.; Vidić, S. Tritium and stable isotope distribution in the atmosphere at the coastal region of Croatia. In *Isotopic Composition of Precipitation in the Mediterranean Basin in Relation to Air Circulation Patterns and Climate*; IAEA-TECDOC-1453; Gourcy, L., Ed.; IAEA: Vienna, Austria, 2005; pp. 37–50.
31. Barešić, J.; Horvatinčić, N.; Krajcar Bronić, I.; Obelić, B.; Vreča, P. Stable Isotope Composition of Daily and Monthly Precipitation in Zagreb. *Isot. Environ. Health Stud.* **2006**, *42*, 239–249. [[CrossRef](#)]
32. Vreča, P.; Krajcar Bronić, I.; Horvatinčić, N.; Barešić, J. Isotopic Characteristics of Precipitation in Slovenia and Croatia: Comparison of Continental and Maritime Stations. *J. Hydrol.* **2006**, *330*, 457–469. [[CrossRef](#)]
33. Brkić, Ž.; Kuhta, M.; Hunjak, T.; Larva, O. Regional Isotopic Signatures of Groundwater in Croatia. *Water* **2020**, *12*, 1983. [[CrossRef](#)]
34. Peel, M.C.; Finlayson, B.L.; McMahon, T.A. Updated World Map of the Köppen-Geiger Climate Classification. *Hydrol. Earth Syst. Sci.* **2007**, *11*, 1633–1644. [[CrossRef](#)]
35. Surić, M.; Lončarić, R.; Lončar, N.; Buzjak, N.; Bajo, P.; Drysdale, R.N. Isotopic Characterization of Cave Environments at Varying Altitudes on the Eastern Adriatic Coast (Croatia)—Implications for Future Speleothem-Based Studies. *J. Hydrol.* **2017**, *545*, 367–380. [[CrossRef](#)]
36. Czappon, G.; Bočić, N.; Buzjak, N.; Óvári, M.; Molnár, M. Monitoring in the Barač and Lower Cerovačka Caves (Croatia) as a Basis for the Characterization of the Climatological and Hydrological Processes That Control Speleothem Formation. *Quat. Int.* **2018**, *494*, 52–65. [[CrossRef](#)]
37. Rudzka, D.; McDermott, F.; Surić, M. A Late Holocene Climate Record in Stalagmites from Modrič Cave (Croatia): Holocene Climate Record from Croatian Stalagmites. *J. Quat. Sci.* **2012**, *27*, 585–596. [[CrossRef](#)]
38. Surić, M.; Lončarić, R.; Bočić, N.; Lončar, N.; Buzjak, N. Monitoring of Selected Caves as a Prerequisite for the Speleothem-Based Reconstruction of the Quaternary Environment in Croatia. *Quat. Int.* **2018**, *494*, 263–274. [[CrossRef](#)]
39. Paar, D.; Mance, D.; Stroj, A.; Pavić, M. Northern Velebit (Croatia) Karst Hydrological System: Results of a Preliminary <sup>2</sup>H and <sup>18</sup>O Stable Isotope Study. *Geol. Croat.* **2019**, *72*, 205–213. [[CrossRef](#)]
40. Lončar, N. Isotopic Composition of the Speleothems from the Eastern Adriatic Islands Caves as an Indicator of Paleoenvironmental Changes. Ph.D. Thesis, University of Zagreb, Zagreb, Croatia, 2012. (In Croatian)

41. Lončar, N.; Bar-Matthews, M.; Ayalon, A.; Faivre, S.; Surić, M. Early and Mid-Holocene environmental conditions in the Eastern Adriatic recorded in speleothems from Mala špilja Cave and Vela špilja Cave (Mljet Island, Croatia). *Acta Carsol.* **2017**, *46*, 229–249. [[CrossRef](#)]
42. Lončar, N.; Bar-Matthews, M.; Ayalon, A.; Faivre, S.; Surić, M. Holocene Climatic Conditions in the Eastern Adriatic Recorded in Stalagmites from Strašna Peć Cave (Croatia). *Quat. Int.* **2019**, *508*, 98–106. [[CrossRef](#)]
43. Surić, M.; Roller-Lutz, Z.; Mandić, M.; Krajcar Bronić, I.; Juračić, M. Modern C, O, and H Isotope Composition of Speleothem and Dripwater from Modrić Cave, Eastern Adriatic Coast (Croatia). *Int. J. Speleol.* **2010**, *39*, 91–97. [[CrossRef](#)]
44. Bogнар, A.; Faivre, S.; Buzjak, N.; Pahernik, M.; Bočić, N. Recent Landform Evolution in the Dinaric and Pannonian Regions of Croatia. In *Recent Landform Evolution*; Lóczy, D., Stankoviansky, M., Kotarba, A., Eds.; Springer: Dordrecht, The Netherlands, 2012; pp. 313–344. [[CrossRef](#)]
45. Hartmann, A.; Gleeson, T.; Rosolem, R.; Pianosi, F.; Wada, Y.; Wagener, T. A Large-Scale Simulation Model to Assess Karstic Groundwater Recharge over Europe and the Mediterranean. *Geosci. Model. Dev.* **2015**, *8*, 1729–1746. [[CrossRef](#)]
46. Bočić, N. Krš—definicija, svojstva, distribucija. In *Speleologija*, 2nd ed.; Rnjak, G., Ed.; Speleološko društvo Velebit, Hrvatski planinarski savez, Hrvatska gorska služba spašavanja: Zagreb, Croatia, 2017; pp. 557–570.
47. Selak, L. Monitoring okolišnih parametara u turistički uređenoj špilji—primjer Baračevih špilja kod Rakovice. Master's Thesis, University of Zagreb, Zagreb, Croatia, February 2019.
48. Paar, D.; Ujević, M.; Bakšić, D.; Lacković, D.; Čop, A.; Radolić, V. Physical and Chemical Research in Velebita Pit (Croatia). *Acta Carsol.* **2008**, *37*, 273–278. [[CrossRef](#)]
49. Paar, D.; Buzjak, N.; Bakšić, D.; Radolić, V. Physical research in Croatia's deepest cave system Lukina jama-Trojama, Mt.Velebit. In Proceedings of the 16th International Congress of Speleology, Brno, Czech Republic, 21–28 July 2013.
50. Paar, D.; Dubovečak, V. Exploration of deep pits of the Northern Velebit National Park. In *Scientific Report for Northern Velebit National Park*; NP Sjeverni Velebit: Krasno, Croatia, 2014; p. 35.
51. Stroj, A.; Paar, D. Water and Air Dynamics within a Deep Vadose Zone of a Karst Massif: Observations from the Lukina Jama–Trojama Cave System (–1431 m) in Dinaric Karst (Croatia). *Hydrol. Process.* **2019**, *33*, 551–561. [[CrossRef](#)]
52. CMHS, 2020 Croatian Meteorological and Hydrological Service.
53. Thornthwaite, C.W. An Approach toward a Rational Classification of Climate. *Geogr. Rev.* **1948**, *38*, 55. [[CrossRef](#)]
54. McCabe, G.J.; Markstrom, S.L. *A Monthly Water-Balance Model Driven by a Graphical User Interface*; USGS Open File Report: Reston, VA, USA, 2007.
55. Domínguez-Villar, D. Heat flux. In *Speleothem Science: From Process to Past Environments*; Fairchild, I.J., Baker, A., Eds.; Wiley-Blackwell: Chichester, UK, 2012; pp. 137–145.
56. Gröning, M.; Lutz, H.O.; Roller-Lutz, Z.; Kralik, M.; Gourcy, L.; Pöhlstein, L. A Simple Rain Collector Preventing Water Re-Evaporation Dedicated for  $\delta^{18}\text{O}$  and  $\delta^2\text{H}$  Analysis of Cumulative Precipitation Samples. *J. Hydrol.* **2012**, *448–449*, 195–200. [[CrossRef](#)]
57. Domínguez-Villar, D.; Lojen, S.; Krklec, K.; Kozdon, R.; Edwards, R.L.; Cheng, H. Ion Microprobe  $\delta^{18}\text{O}$  Analyses to Calibrate Slow Growth Rate Speleothem Records with Regional  $\delta^{18}\text{O}$  Records of Precipitation. *Earth Planet. Sci. Lett.* **2018**, *482*, 367–376. [[CrossRef](#)]
58. Baker, A.; Barnes, W.; Smart, P. Variations in the discharge and organic matter content of stalagmite drip waters in Lower Cave, Bristol. *Hydrol. Process.* **1997**, *11*, 1541–1555. [[CrossRef](#)]
59. Collister, C.; Matthey, D. High Resolution Measurement of Water Drip Rates in Caves Using an Acoustic Drip Counter. *AGU Fall Meet.* **2005**, *31*.
60. Scholz, D.; Frisia, S.; Borsato, A.; Spötl, C.; Fohlmeister, J.; Mudelsee, M.; Miorandi, R.; Mangini, A. Holocene Climate Variability in North-Eastern Italy: Potential Influence of the NAO and Solar Activity Recorded by Speleothem Data. *Clim. Past* **2012**, *8*, 1367–1383. [[CrossRef](#)]
61. Wassenburg, J.A.; Immenhauser, A.; Richter, D.K.; Niedermayr, A.; Riechelmann, S.; Fietzke, J.; Scholz, D.; Jochum, K.P.; Fohlmeister, J.; Schröder-Ritzrau, A.; et al. Moroccan Speleothem and Tree Ring Records Suggest a Variable Positive State of the North Atlantic Oscillation during the Medieval Warm Period. *Earth Planet. Sci. Lett.* **2013**, *375*, 291–302. [[CrossRef](#)]

62. Baker, A.; Hellstrom, J.; Kelly, B.F.J.; Mariethoz, G.; Trouet, V. A Composite Annual-Resolution Stalagmite Record of North Atlantic Climate over the Last Three Millennia. *Sci. Rep.* **2015**, *5*, 10307. [[CrossRef](#)]
63. Luetscher, M.; Boch, R.; Sodemann, H.; Spötl, C.; Cheng, H.; Edwards, R.L.; Frisia, S.; Hof, F.; Müller, W. North Atlantic Storm Track Changes during the Last Glacial Maximum Recorded by Alpine Speleothems. *Nat. Commun.* **2015**, *6*, 6344. [[CrossRef](#)]
64. Gat, J.R.; Carmi, I. Effect of climate changes on the precipitation patterns and isotopic composition of water in a climate transition zone: Case of the Eastern Mediterranean Sea area. In *The Influence of Climate Change and Climatic Variability on the Hydrologic Regime and Water Resources, Proceedings of the Vancouver Symposium, Vancouver, Canada, August 1987*; IAHS Publication: Vancouver, WA, Canada; pp. 513–523.
65. Gat, J.R.; Klein, B.; Kushnir, Y.; Roether, W.; Wernli, H.; Yam, R.; Shemesh, A. Isotope Composition of Air Moisture over the Mediterranean Sea: An Index of the Air-Sea Interaction Pattern. *Tellus B Chem. Phys. Meteorol.* **2003**, *55*, 953–965. [[CrossRef](#)]
66. Dansgaard, W. Stable Isotopes in Precipitation. *Tellus* **1964**, *16*, 436–468. [[CrossRef](#)]
67. Celle-Jeanton, H.; Travi, Y.; Blavoux, B. Isotopic Typology of the Precipitation in the Western Mediterranean Region at Three Different Time Scales. *Geophys. Res. Lett.* **2001**, *28*, 1215–1218. [[CrossRef](#)]
68. Clark, I.D.; Fritz, P. *Environmental Isotopes in Hydrogeology*, 1st ed.; CRC Press: Boca Raton, FL, USA, 1997. [[CrossRef](#)]
69. Yonge, C.J.; Ford, D.C.; Gray, J.; Schwarcz, H.P. Stable Isotope Studies of Cave Seepage Water. *Chem. Geol. Isot. Geosci. Sect.* **1985**, *58*, 97–105. [[CrossRef](#)]
70. Bar-Matthews, M.; Ayalon, A.; Matthews, A.; Sass, E.; Halicz, L. Carbon and Oxygen Isotope Study of the Active Water-Carbonate System in a Karstic Mediterranean Cave: Implications for Paleoclimate Research in Semiarid Regions. *Geochim. Cosmochim. Acta* **1996**, *60*, 337–347. [[CrossRef](#)]
71. Van Beynen, P.; Febroriello, P. Seasonal Isotopic Variability of Precipitation and Cave Drip Water at Indian Oven Cave, New York. *Hydrol. Process.* **2006**, *20*, 1793–1803. [[CrossRef](#)]
72. Beddows, P.A.; Mandić, M.; Ford, D.C.; Schwarcz, H.P. Oxygen and Hydrogen Isotopic Variations between Adjacent Drips in Three Caves at Increasing Elevation in a Temperate Coastal Rainforest, Vancouver Island, Canada. *Geochim. Cosmochim. Acta* **2016**, *172*, 370–386. [[CrossRef](#)]
73. Markowska, M.; Baker, A.; Treble, P.C.; Andersen, M.S.; Hankin, S.; Jex, C.N.; Tadros, C.V.; Roach, R. Unsaturated Zone Hydrology and Cave Drip Discharge Water Response: Implications for Speleothem Paleoclimate Record Variability. *J. Hydrol.* **2015**, *529*, 662–675. [[CrossRef](#)]
74. White, W.B. Conceptual models for karstic aquifers. In *Karst Modelling: Special Publication 5*; Palmer, A.N., Palmer, M.V., Sasowsky, I.D., Eds.; Karst Waters Institute Special Publication, The Karst Waters Institute: Charles Town, WV, USA, 1999; pp. 11–16.
75. Ford, D.; Williams, P. *Karst Hydrogeology and Geomorphology*; John Wiley & Sons: Chichester, UK, 2007; p. 578.
76. Smart, P.L.; Friedrich, H. Water movement and storage in the unsaturated zone of a maturely karstified aquifer, Mendip Hills, England. In *Proceedings of the Environmental Problems in Karst Terrains and Their Solutions Conference, Bowling Green, KY, USA, 28–30 October 1986*; National Water Well Association: Bowling Green, KY, USA, 1987; pp. 57–87.
77. Baker, A.; Hartmann, A.; Duan, W.; Hankin, S.; Comas-Bru, L.; Cuthbert, M.O.; Treble, P.C.; Banner, J.; Genty, D.; Baldini, L.M.; et al. Global Analysis Reveals Climatic Controls on the Oxygen Isotope Composition of Cave Drip Water. *Nat. Commun.* **2019**, *10*, 2984–2987. [[CrossRef](#)]
78. Buzjak, N.; Bočić, N.; Paar, D.; Bakšić, D.; Dubovečak, V. Ice Caves in Croatia. *Ice Caves* **2018**, 335–369. [[CrossRef](#)]
79. Sharp, Z. *Principles of Stable Isotope Geochemistry*, 1st ed.; Pearson Prentice Hall: Upper Saddle River, NJ, USA, 2007.
80. Rozanski, K.; Araguás-Araguás, L.; Gonfiantini, R. Isotopic patterns in modern global precipitation. *Geoph. Monog.* **1993**, *78*, 1–36.
81. Johnston, V.E.; Borsato, A.; Spötl, C.; Frisia, S.; Miorandi, R. Stable isotopes in caves over altitudinal gradients: Fractionation behaviour and inferences for speleothem sensitivity to climate change. *Clim. Past* **2013**, *9*, 99–118. [[CrossRef](#)]
82. Nehme, C.; Verheyden, S.; Nader, F.H.; Adjizian-Gerard, J.; Genty, D.; De Bondt, K.; Minster, B.; Salem, G.; Verstraten, D.; Clayes, P. Cave dripwater isotopic signals related to the altitudinal gradient of Mount-Lebanon: Implication for speleothem studies. *Int. J. Speleol.* **2019**, *48*, 63–74. [[CrossRef](#)]

83. Coplen, T.B.; Kendall, C.; Hopple, J. Comparison of stable isotope reference samples. *Nature* **1983**, *302*, 236–238. [[CrossRef](#)]
84. Tremaine, D.M.; Froelich, P.N.; Wang, Y. Speleothem calcite formed in situ: Modern calibration of  $\delta^{18}\text{O}$  and  $\delta^{13}\text{C}$  paleoclimate proxies in a continuously-monitored natural cave system. *Geochim. Cosmochim. Acta* **2011**, *75*, 4929–4950. [[CrossRef](#)]
85. Daëron, M.; Drysdale, R.N.; Peral, M.; Huyghe, D.; Blamart, D.; Coplen, T.B.; Lartaud, F.; Zanchetta, G. Most Earth-surface calcites precipitate out of isotopic equilibrium. *Nat. Commun.* **2019**, *10*, 429. [[CrossRef](#)]
86. Friedman, I.; O’Neil, J.R. Compilation of stable isotope fractionation factors of geochemical interest. In *Data of Geochemistry*, 6th ed.; Fleisher, M., Chap, K.K., Eds.; US Geological Survey Professional Paper: Washington, DC, USA, 1977; Volume 440, pp. 1–12.
87. Coplen, T.B. Calibration of the calcite-water oxygen-isotope geothermometer at Devils Hole, Nevada, a natural laboratory. *Geochim. Cosmochim. Acta* **2007**, *71*, 3948–3957. [[CrossRef](#)]
88. Mandić, M.; Bojić, D.; Roller-Lutz, Z.; Lutz, H.O.; Krajcar Bronić, I. Note on the spring region of Gacka River (Croatia). *Isot. Environ. Health S.* **2008**, *44*, 201–208. [[CrossRef](#)]
89. Czuppon, G.; Demény, A.; Leél-Óssy, S.; Óvari, M.; Molnár, M.; Stieber, J.; Kármán, K.; Kiss, K.; Haszpra, L. Cave monitoring in Béke and Baradla Caves (NE Hungary): Implications for condition of formation cave carbonates. *Int. J. Speleol.* **2018**, *47*, 13–28. [[CrossRef](#)]
90. Drysdale, R.N.; Hellstrom, J.; Zanchetta, G.; Fallick, A.; Goñi, M.F.S.; Couchoud, I.; McDonald, J.; Maas, R.; Lohmann, G.; Isola, I. Evidence for obliquity forcing of glacial termination II. *Science* **2009**, *325*, 1527–1531. [[CrossRef](#)]



© 2020 by the authors. Licensee MDPI, Basel, Switzerland. This article is an open access article distributed under the terms and conditions of the Creative Commons Attribution (CC BY) license (<http://creativecommons.org/licenses/by/4.0/>).